16 State House Station
Augusta, Maine 04333

MaineDOT

Transportation Research Division



Technical Report 14-07

Advanced Bridge Safety Initiative

Task 3: Slab Bridge Load Rating using AASHTO Methodology and Finite Element Analysis – An Analysis of 20 Bridges & Guidelines

Final Report – Task 3, December 2011

Technical Report Documentation Page

1. Report No. ME 14-07	2.	3. Recipient's Accession No.	
4. Title and Subtitle Slab Bridge Load Rating using AASHTO Methodology and Finite Element Analysis – An Analysis of 20 Bridges		5. Report Date December 2011 6.	
7. Author(s) Timothy J. Poulin Bill Davids, Ph.D., P.E.		8. Performing Organization Report No.	
9. Performing Organization Name and Address University of Maine		10. Project/Task/Work Unit No. Project 017666.00 Task 3 11. Contract © or Grant (G) No. Contract # 20100506*5729	
12. Sponsoring Organization Name and Address Maine Department of Transportation 16 State House Station Augusta, Maine 04333		13. Type of Report and Period Covered 14. Sponsoring Agency Code	
15. Supplementary Notes			

16. Abstract (Limit 200 words)

Current AASHTO provisions for the conventional load rating of flat slab bridges rely on the equivalent strip method of analysis for determining live load effects, this is generally regarded as overly conservative by many professional engineers. As a result there are a significant number of slab bridges in Maine that are (or will be) posted for reduced truck weights, when in reality such postings may not be necessary.

In Tasks 1 and 2 of this study a program called SlabRate is developed and validated. SlabRate computes the rating factors for simply-supported, continuous flat slab bridges using finite element analysis (FEA).

This report under Task 3 explores the potential benefits of using SlabRate over the conventional strip width, twenty existing bridges were load rated using both. Twenty one different truck configurations were analyzed, these include AASHTO's design and legal trucks, along with AASHTO's specialized hauling vehicles and MaineDOT's rating trucks.

It was also concluded that SlabRate can be reliably used to load rate flat slab bridges having skew angles of 20° or less. Only fourteen bridges of the original twenty bridges met this criteria, of which seven would have rating factors above one using SlabRate while below one using the conventional strip width method.

17. Document Analysis/Descriptors Concrete slab bridges, load rating, finite element analysis		18. Availability Statement	
19. Security Class (this report)	20. Security Class (this page)	21. No. of Pages 93	22. Price

Slab Bridge Load Rating Using AASHTO Methodology and Finite-Element Analysis

Prepared for the Maine Department of Transportation
Dec. 31, 2011

William G. Davids, PhD, PE
John C. Bridge Professor of Civil and Environmental Engineering

Timothy Poulin, Graduate Student
Department of Civil and Environmental Engineering and the AEWC Advanced Structures and Composites Laboratory

1 Background

Following the I-35 Minnesota bridge failure, Governor Baldacci issued an Executive Order directing the Maine Department of Transportation (MaineDoT) to review Maine's bridge inspection and programming. The Advanced Bridge Safety Program has been designed to address recommendations from the MaineDoT report titled "Keeping Our Bridges Safe" (MaineDoT 2007).

The MaineDoT is responsible for 2,723 bridges and minor spans, of which 271 are in poor condition and 226 are structurally deficient. Nine percent of Maine's bridges are over 81 years old and 37% are over 61 years old. The MaineDoT estimates that 288 bridges are at risk of closure or weight restrictions in the next decade.

Closing or restricting a bridge places additional hardships on Maine people and Maine companies. The MaineDoT struggles to balance public safety and socioeconomic concerns when faced with bridge closure and load restriction decisions. On the other hand, the cost of replacement or rehabilitation needed to keep such a bridge open to all traffic is extraordinary.

The magnitude of this issue is highlighted in the report titled "Keeping Our Bridges Safe" (MaineDoT 2007). The report concludes that between 30 and 40 bridges need to be replaced each year over the coming decade to reduce additional bridge closures or restrictions. With additional rehabilitation costs, the report estimates that funding for bridge replacement and rehabilitation needs to be increased from $70M/year to $130M/year to ensure bridge safety and minimize bridge restrictions or closures. Subsequent to the report, the Legislature increased funding substantially but short of meeting the needs. They are relying on MaineDoT to continue to find innovations to address this significant problem.

This report examines this issue through the use of FE analysis methods for load-rating concrete slab and rigid frame bridges. The objective of this report is to show the potential benefits of advanced analysis methods. Current AASHTO provisions for the conventional load rating of slab bridges rely on the equivalent strip method of analysis for determining live load effects (AASHTO 2009), which has been shown to be conservative compared to more advanced analysis methods (Jáuregui et al. 2007). As a result, there are a significant number of slab bridges in Maine that could require posting for reduced truck weights, when in reality such postings may not be necessary. Recent research conducted in New Mexico (Jáuregui et al. 2007) examined this issue, and found that an 11% - 26% increase in live load capacity for a multi-span slab bridge was justified based on advanced analysis. This report specifically examines the use of FE analysis methods for load-rating concrete slab bridges in Maine.

2 Conventional Strip Width Method

The current American Association of State Highway and Transportation Officials (AASHTO) Manual for Bridge Evaluation (AASHTO 2009) uses the equivalent strip width method for calculating live load effects in slab bridges, and provides guidelines to load rate existing bridges according to the equivalent strip width method. These load rating guidelines are what the MaineDoT currently follows for load rating bridges. The general load rating equation is still used for the finite element model. However, the finite element model is used to determine slab bending moments within the bridge instead of the conventional strip width method. The general load rating equations used with both the finite element results and the conventional strip width method are shown below in equations 1-3 (AASHTO 2009, Equation 6A.4.2.1 -1, 6A.4.2.1 -2, 6A.4.2.1 -3 respectivly):

$$RF = \frac{C - (\gamma_{DC})(DC) - (\gamma_{DW})(DW) - (\gamma_P)(P)}{(\gamma_{LL})(LL + IM)} \qquad \text{Equation 1}$$

For Strength Limit States:

$$C = R_n \varphi_c \varphi_s \varphi$$ Equation 2

And the following lower limit applies:

$$\varphi_c \varphi_c \geq 0.85$$ Equation 3

Where:

RF = Rating Factor

C = Capacity

DC = Dead load effect due to structural components and attachments

DW = Dead load effect due to wearing surface and utilities

P = Permanent loads other than dead loads

LL = Live load effect

IM = Dynamic load effect (impact)

γ_{DC} = LRFD load factor for structural components and attachments

γ_{DW} = LRFD load factor for wearing surface and utilities

γ_P = LRFD load factor for permanent loads other than dead loads

γ_{LL} = Evaluation live load factor

φ_c = Condition factor

φ_s = System Factor

φ = LRFD resistance factor

R_n = Nominal Member Resistance

To determine the equivalent strip width, section 4.6.2.3 of the 2010 AASHTO LRFD Bridge Design Specifications (AASHTO 2010) is used. The maximum moments for a wheel line are then determined for the bridge by modeling the bridge has a beam, either continuous or single span depending on the bridge, and that moment is then distributed over the equivalent strip width to get a moment per unit width. The equivalent strip is taken as the minimum of the equivalent strip width for one lane loaded or for multiple lanes of loading. The equations to determine the strip width are shown below in equations 4-5 (AASHTO 2010, Equation 4.6.2.3-1, 4.6.2.3-1 respectively):

For one lane of loading:

$$E = 250 + 0.42\sqrt{L_1 W_1} \qquad \text{Equation 4}$$

For multiple lanes of loading:

$$E = 2100 + 0.12\sqrt{L_1 W_1} \le \frac{W}{N_L} \qquad \text{Equation 5}$$

Where:

E = Equivalent width (mm)

L_1 = Modified span length taken equal to the lesser of the actual span or 18000 (mm)

W_1 = Modified edge-to-edge width of bridge taken to be equal to the lesser of the actual width or 18000 for multilane loading, or 9000 for single-lane loading (mm)

W = physical edge to edge width of bridge (mm)

N_L = Number of design lane as specified in Article 3.6.1.1.1

For skewed bridge, the longitudinal force effects may be reduced by the factor *r* given in Equation 6 (AASHTO 2010, Equation 4.6.2.3 -3)*:*

$$r = 1.05 - 0.25\tan\theta \leq 1.00 \qquad \text{Equation 4.6.2.3 – 3}$$

Where:

θ = Skew angle (degrees)

3 SlabRate Finite Element Program

The finite element program SlabRate was created using MATLAB (MathWorks 2009) for the load rating of continuous flat slab bridges with one to five spans. SlabRate automatically generates multiple lanes of live loading, allows the definition of a variety of dead loads, and displays a summary of load rating results in the Graphical User Interface (GUI) and an Excel file, and gives detailed ASCII text file output for each rating vehicle. The following sections describe the underlying finite element modeling approach, live loading assumptions and rating factor calculations.

3.1 Finite Element Modeling Approach

3.1.1 Finite Element Theory and Calculations

The underlying finite element model relies on an 8-noded, shear deformable plate element. This element is described in detail in Bhatti (2006). Quadratic shape functions are used for element displacements. To avoid shear locking, the shear contributions to the element stiffness matrix are under-integrated using 2x2 Gaussian quadrature; 3x3 Gaussian quadrature is used for integrating the bending contributions to the element stiffness matrix. An isoparametric element formulation allows the use of non-rectangular elements, which are required when modeling bridges with

skewed supports. After solving for displacements and computing the corresponding moments in each element, nodal averaging of the moments is automatically performed.

The finite element mesh is uniform, although different numbers of elements in the traffic direction may be used for each span (see Figure 1 for a plan view of mesh of a 4-span bridge). A single element width is usually assumed under each curb and a single element width is generally used between the face of each curb and the nearest wheel line. (More element widths under the curbs and between the curb face and nearest wheel line may be used to maintain good element aspect ratios.) The global coordinate system used in the model definition and in model output has its origin centered on the left-most pier, with *x* positive to the right and *y* positive upward as shown in Figure 1. Pinned supports are assumed at all piers.

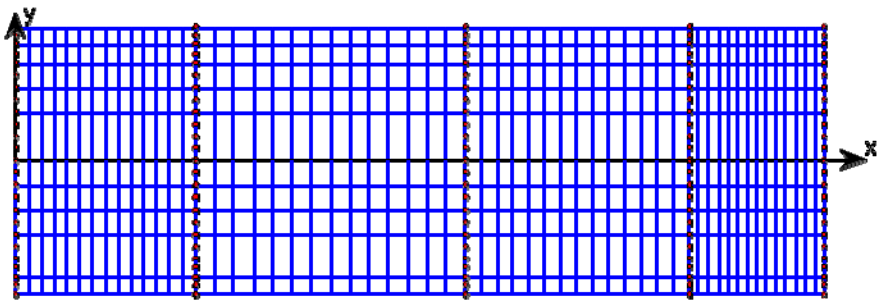

Figure 1 - Mesh of Four-Span Continuous Slab Bridge

3.1.2 General Load Application

To allow the straightforward analysis for multiple truck positions and a variety of dead loads at any position on the bridge, moment influence coefficients are generated for each node in the model. Using the nodal influence coefficients, moments due to a load at any point in the model may then be easily computed. The mesh is triangulated using a Delaunay triangulation to permit a point load at any point on the deck surface to be easily distributed to the three nodes defining the triangle in which the point load lies. In turn, this allows a uniform patch load to be treated as the

sum of a large number of smaller point loads with no need for the finite element mesh and the load patch to be coincident.

3.1.3 Application of Live Loads

Live loads may consist of a truck and a lane load. The maximum number of lanes that will fit on the traveled width is automatically computed, and the bridge is analyzed from one to this maximum number of loaded lanes. Each lane is positioned at multiple locations along the span and across the bridge, including positioning lanes as close as possible to the top and bottom curbs. The truck direction is always left-to-right, but the axle order is automatically run both as defined for the truck and reversed to capture the effect of different travel directions. When loading multiple lanes for a bridge with non-skewed abutments, adjacent trucks are assumed to be in the same *x*-position. For bridges with skewed abutments, the *x*-position of adjacent trucks is varied along the span based on the abutment skew angles, which produces larger moments in the slab. Truck axles that do not contribute to the maximum load effect may be either considered or dropped at the option of the user.

Each wheel load is treated as a 25.4 cm x 50.8 cm uniform pressure, which is divided into an 8x16 grid of squares. The uniform pressure acting over each of these 128 squares is then converted to an individual point load, and the moments produced by each point load are determined using pre-computed influence coefficients as detailed previously.

Lane loads are treated as uniform loads acting over a 3.05 m loaded width positioned transversely within each lane to maximize their effect. Load patterns are automatically generated where all possible combinations of alternate spans are loaded to maximize positive moment, and adjacent spans plus alternate spans are loaded to maximize negative moments at interior piers.

Individual truck loads (including any lane load and the live load factor) are defined in ASCII input files. All HL-93 loadings, AASHTO rating vehicles (operating and inventory level) and

legal loads, and MaineDoT rating vehicles and legal loads are pre-defined. Additional trucks may easily be created using the same format used in these files. Axle positions are assumed fixed for all trucks.

3.1.4 Application of Dead Loads

Dead loads are treated as uniform pressures or uniform line loads. In addition to slab self-weight, the wearing surface, curbs and railings are explicitly considered. Any number of additional uniform line loads may be specified to account for interior barriers, utilities, etc.

3.2 SlabRate Validation

3.2.1 Verification of Isoparametric Finite Element Implementation

The finite element implementation – including the generation of the structural stiffness matrix, calculation of influence coefficients, and load application using the mesh triangulation detailed above – was verified by computing displacement and moment at the center of a uniformly loaded, simply-supported square plate. The plate dimensions are 254 cm by 254 cm by 10.2 cm thick with an elastic modulus of 68950 MPa and a Poisson's ratio of 0.3. Under a uniform pressure of 0.689 MPa, the deflection at the center of the plate is 1.76 cm and the maximum moment is 5.41 kN-m per Timoshenko and Woinowski-Krieger (1959). This solution assumes that there are no shear deflections.

The same plate was modeled with the finite element code and 8-noded plate elements underlying SlabRate. To ensure negligible shear deflections, the shear modulus was set to 6.89×10^9 MPa. Four different analyses were completed with meshes of 4x4, 8x8, 12x12 and 16x16 elements. Table 1 below summarizes the results of the analyses and shows the percent error compared with the analytical solution. The results are in excellent agreement with the analytical solution even with the coarsest mesh. The displacement is likely converging to a value slightly greater than the

analytical solution due to shear deflections that are not entirely eliminated by use of an artificially large value for the shear modulus.

Table 1 - Comparison of FE and Analytical Solutions for a Simply-Supported Plate

Mesh	FE Moment (kN – m)	Moment Error	FE Displacement (cm)	Displacement Error
4x4	5.42	0.19%	1.72	2.51%
8x8	5.40	0.20%	1.76	0.68%
12x12	5.40	0.09%	1.77	0.67%
16x16	5.40	0.11%	1.78	0.85%

An additional test was performed to verify the model's ability to accurately predict response with distorted elements. The same simply-supported plate was modeled with a mesh having the element corner nodes randomly perturbed in both coordinate directions assuming a uniform distribution of +/-25% of the square element edge length. The center node and the edge nodes of the plate were not perturbed so that the plate remained square and results could be recovered at the center of the plate. Figure 2 shows a typical perturbed 12x12 mesh which resulted in a predicted maximum displacement at the center of the plate of 1.77 cm and a predicted maximum moment of 5.40 kN-m. These values agree very well with the analytical solution, verifying the proper implementation of the isoparametric formulation for non-rectangular elements.

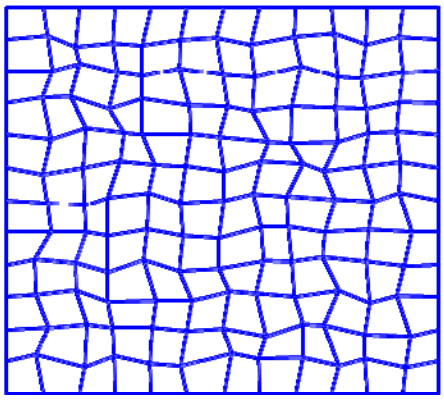

Figure 2 - Distorted Mesh of Simply-Supported Rectangular Plate

3.2.2 Bending Moments in a Two-Span Continuous Slab

To further test the accuracy of the formulation and application of boundary conditions, a continuous, simply-supported slab bridge with two equal spans of 12.2 m each was modeled. The overall slab width was 9.14 m, and a 5.08 cm thick wearing surface weighing 2240 kg/m^3 was specified. The finite element mesh used in these simulations had 16 elements longitudinally per span, and 10 elements perpendicular to the span direction.

Under a uniform load, a continuous beam with two equal spans has a maximum negative moment at the interior pier of $wl^2/8$, where w = the uniform load (kN/m) and l = the length of one span. With a slab unit weight of 2400 kg/m^3, this calculation gives a slab self-weight moment of 200 kN-m/m, and the moment due to the wearing surface is similarly computed as 18.0 kN-m/m. The finite element model predicted average moments across the center pier of 201 kN-m/m and 17.70 kN-m/m, respectively, which agree very well with the theoretical hand-calculated values.

3.2.3 Truck Live Load Moments for a Simple Span

To verify the previously defined method of live load application, live load moments were computed using the HL-93 truck and the AASHTO rating vehicles for a 24.38 m simple span bridge. The long span was used to ensure that all or most of the truck axles contributed to the

mid-span moment. The finite element model had 16 elements in both the longitudinal and transverse direction. The bridge width was 9.75 m and each curb width was taken as 61.0 cm, which conveniently yields a 61.0 cm width for each element in the model. The total moment at mid-span was computed by numerically integrating the model-predicted moments per linear foot across the width of the bridge using the trapezoidal rule assuming moments varied linearly across the width of each element. These model-computed moments were then compared with the moments given in AASHTO (2008) for a 24.38 m simple span. As shown in Table 2 below, the model-computed moments are in excellent agreement with the values given by AASHTO.

Table 2 - Comparison of LL Moments per AASHTO and LL Moments Computed with SlabRate

Truck	Moment per AASHTO (kN-m)	Moment predicted by FE code (kN-m)	Error (%)
HL-93 (truck only)	2116	2091	-1.2
Type 3	1529	1528	-0.09
Type 3-S2	1757	1733	-1.4
Type 3-3	1702	1689	-0.72
NRL	2411	2421	0.45
SU4	1708	1710	0.08
SU5	1899	1897	-0.14
SU6	2116	2110	-0.32
SU7	2317	2320	0.12

3.3 SlabRate Convergence Study for Non-Skewed Bridges

Before any finite element load ratings were completed, a mesh refinement study was done to determine how many elements are needed in both the longitudinal and transverse directions for bridges with no skew. A mesh size needs to be found such that the rating factors and live load moments have converged to a relatively constant value. For this convergence study two bridges were analyzed: Argyle Township Bridge #3827 and Levant Bridge #5253.

The bridge characteristics used in this convergence study can be seen in Table 3. Concrete compressive strength of 17.23 MPa and steel reinforcing yield strength of 227 MPa were used for both bridges. An elastic modulus of 19640 MPa was also used for both bridges along with a Poisson's ratio of 0.19 and a unit weight of concrete of 2400 kg/m^3. The rail weights are modeled as constant distributed load, this distributed load was determined by finding the maximum moment due to the real rail weights than determining the constant distributed load that would provide the same maximum moment.

Table 3 – Bridge Characteristics for Bridges used in the Convergence Study for Non-Skewed Bridges for SlabRate.

Bridge	Argyle Township #3827	Levant Bridge #5253
Span Length (m)	6.664	8.115
Bridge Width (m)	8.434	7.824
Slab Thickness (m)	0.406	0.470
Wearing Surface Thickness (m)	0.102	0.102
Moment Resistance (kN-m / m)	288.7	307.12
Rail Weights (kN/m) (Top / Bottom)	2.810 / 2.810	0.898 / 0.898
Top Curb Height / Width (m)	0.330 / 0.343	0.305 / 0.559
Bottom Curb Height / Width (m)	0.330 / 0.343	0.305 / 0.559
Striped Lane Offset (m) (Top / Bottom)	0.914 / 1.041	0.610 / 0.610

An HL-93 truck and tandem, along with lane loads, were used in the analysis. The number of longitudinal elements tested in this convergence study ranged from 6 to 22 elements in increments of 4 elements. For each of the different longitudinal meshes sizes the number of the transverse elements also ranged from 6 to 22. The live load moments on the Argyle Township Bridge #3827 are shown in Figures 3 and 4 below:

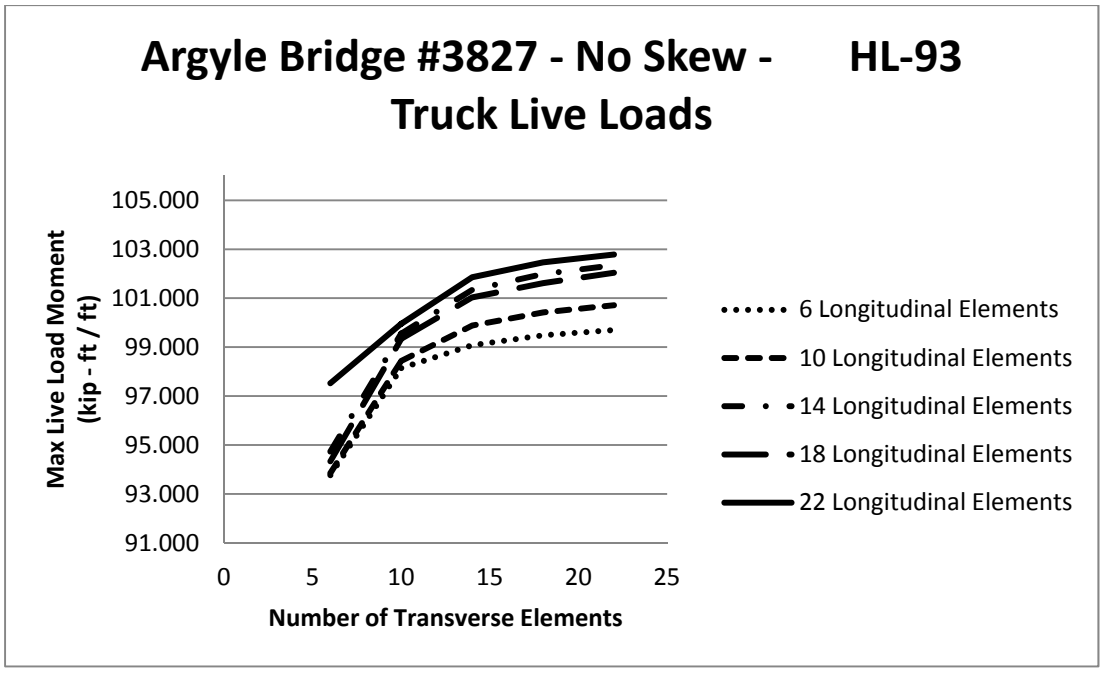

Figure 3 - Affects on Max Live load Moment with an Increase in Mesh Elements under HL-93 Truck and Lane Load for Argyle Township Bridge #3827.

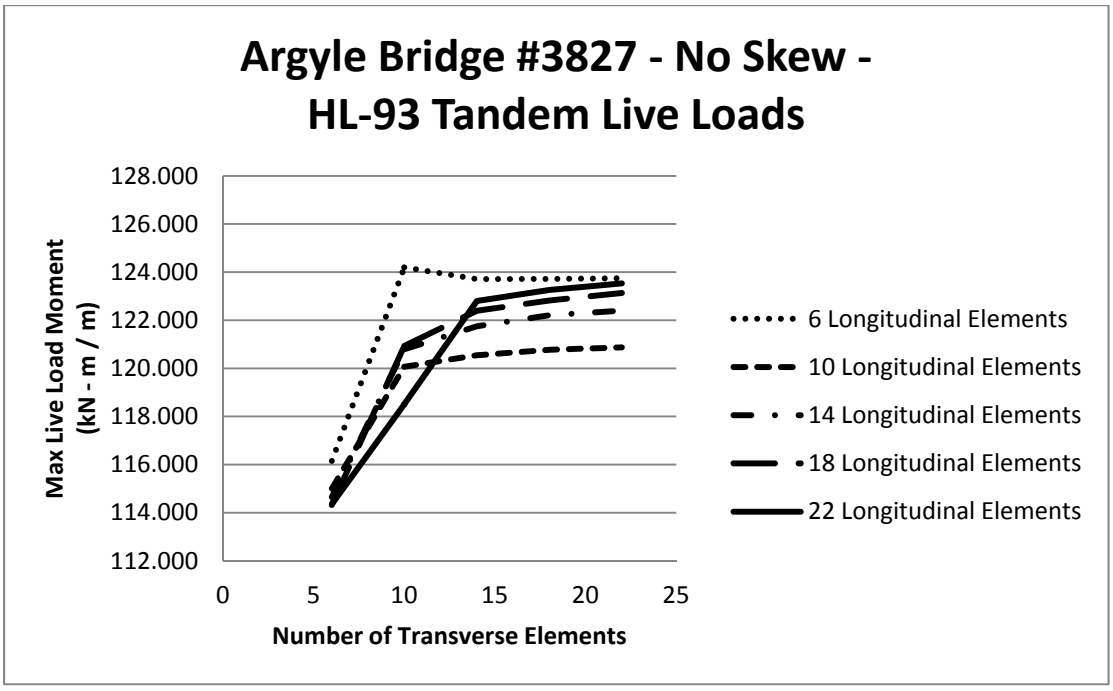

Figure 4- Affects on Max Live load Moment with an Increase in Mesh Elements under HL-93 Tandem and Lane Load for Argyle Township Bridge #3827.

As seen in Figures 3 - 4, both the number of longitudinal and transverse elements have an effect on the maximum live load determined from the FEA model SlabRate. The graphs show that the live load moment for both HL-93 truck and tandem, both with lane load, converge to a relatively constant value at 14 longitudinal and 14 transverse elements. A difference in live load moment of 2.3% and 1.6% are seen from 6 to 14 longitudinal for HL-93 truck and HL-93 tandem loads respectively, both with 14 transverse elements. Only a 0.5% and 0.8% difference from 14 to 22 longitudinal elements was seen for HL-93 truck and tandem load, respectively. There is a 7.0% difference for HL-93 truck load and 6.2% difference for HL-93 tandem load while going from 6 to 14 transverse elements while 14 longitudinal elements are used, and only 1.0% and 0.5% differences are seen between 14 and 22 transverse elements.

Levant Bridge #5253 maximum live load moments follow the same pattern as Argyle Bridge #3827, Figures 5 – 6 show the maximum live load moments for Levant Bridge #5253. The bridge appears to converge to a relatively constant value when 10 longitudinal and 10 transverse elements are used. Since Argyle Bridge #3827 converged to a relatively constant value while using 14 longitudinal and 14 transverse elements, the study will show the difference up to and after using 14 elements. Levant Bridge #5253 sees a difference in live load moment of 9.2% and 2.5% when increasing from 6 to 14 longitudinal for HL-93 truck and HL-93 tandem respectively, both including lane load. While only a 1.4% and 0.3% difference for HL-93 truck and HL-93 tandem load respectively while increasing the number of longitudinal elements from 14 to 22. When increasing the number transverse elements from 6 to 14 an increase of 7.0% and 6.2% in live load moment was seen for HL-93 truck and tandem loads respectively. While only a 1.3% and 0.9% difference were seen between 14 and 22 transverse elements.

Figures 7 – 10 show the rating factors for Argyle Township Bridge #3827 for the HL-93 truck and tandem live loads for different mesh sizes. The rating factors for both loading cases for both inventory and operating follow the same pattern as the live load moments. They also show that

the rating factors converge to a relatively constant value when 14 longitudinal and 14 transverse elements are used. This is because the dead load moments are remaining relatively constant irrespective of mesh refinements, so changes in live load moment are the primary driver of changes in the rating factor. Analyses of several bridges – both skewed and non-skewed – provide similar results, and therefore the remainder of the convergence studies will examine only live load moments.

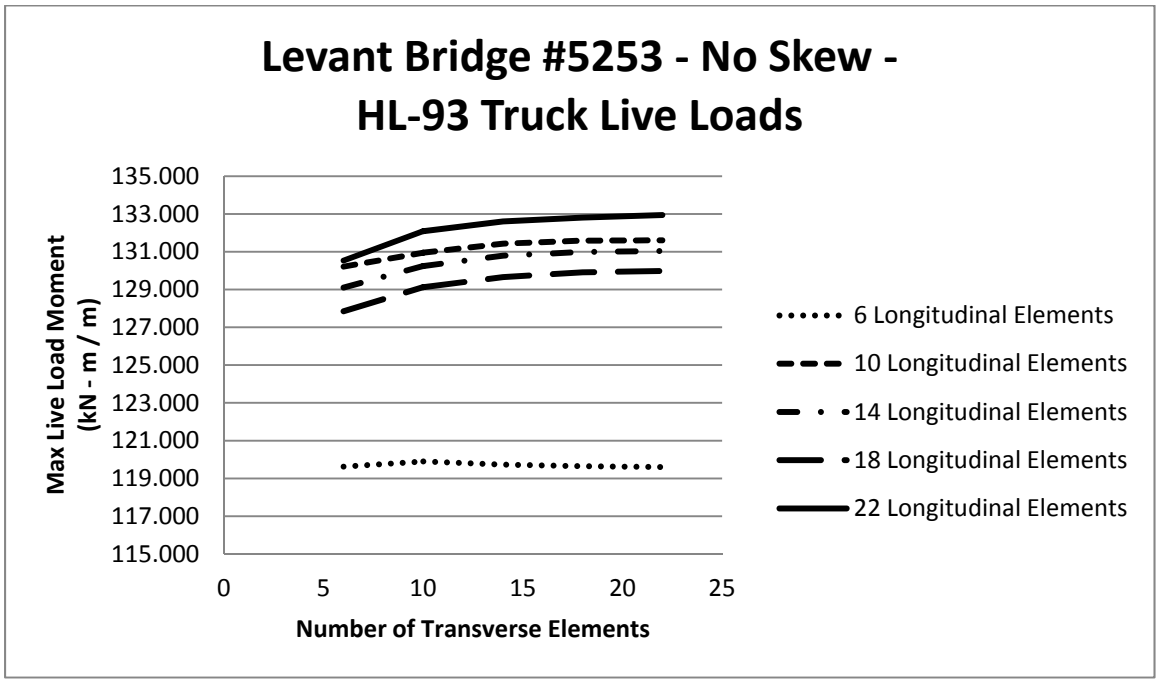

Figure 5 - Effects on Max Live load Moment with an Increase in Mesh Elements under HL-93 Truck and Lane Load for Levant Bridge #5253.

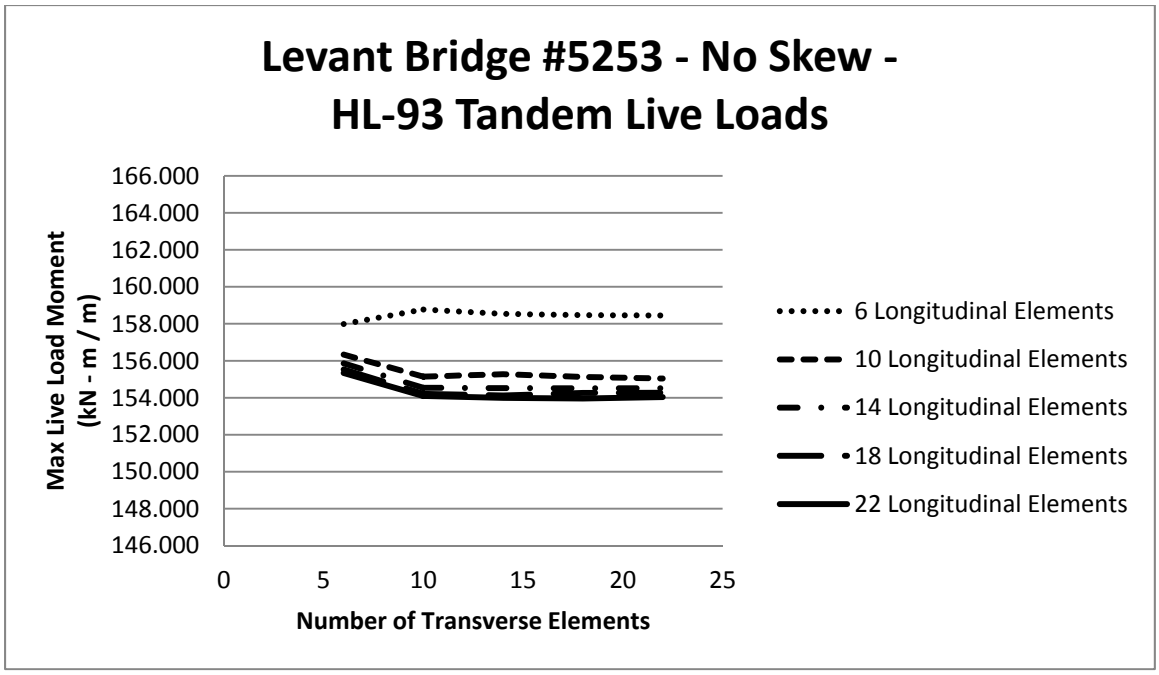

Figure 6 - Effects on Max Live load Moment with an Increase in Mesh Elements under HL-93 Tandem and Lane Load for Levant Bridge #5253.

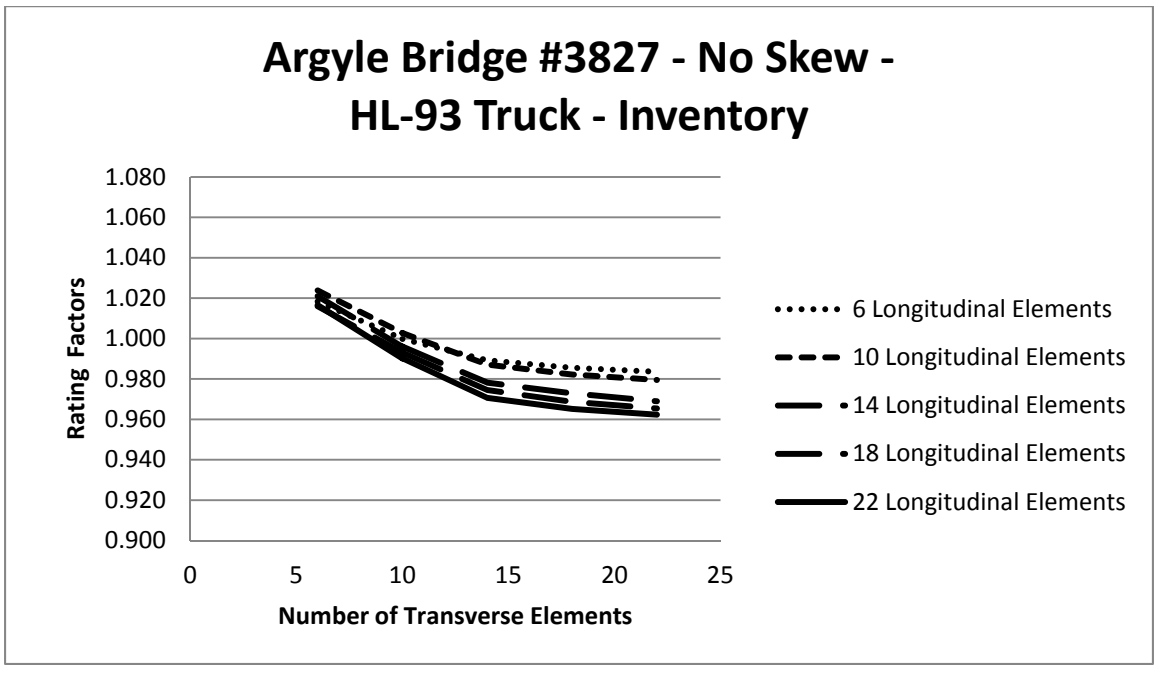

Figure 7 - Effects on Inventory Rating Factor with an Increase in Mesh Elements under HL-93 Truck and Lane Load for Argyle Township Bridge #3827.

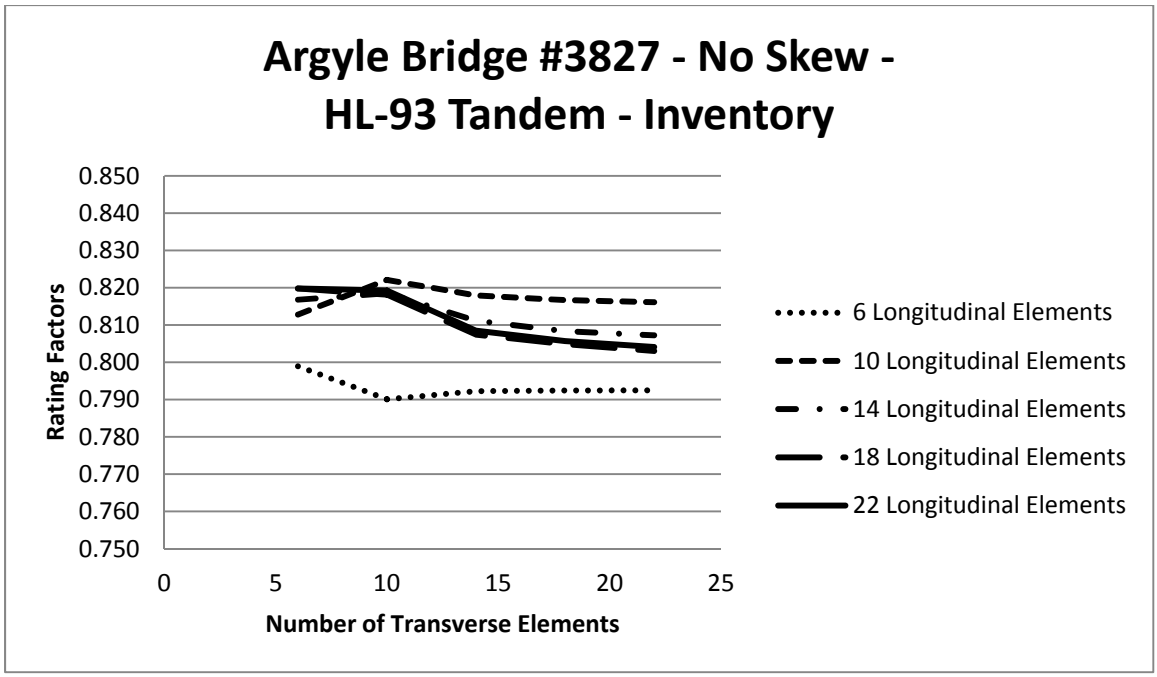

Figure 8 - Effects on Inventory Rating Factor with an Increase in Mesh Elements under HL-93 Tandem and Lane Load for Argyle Township Bridge #3827.

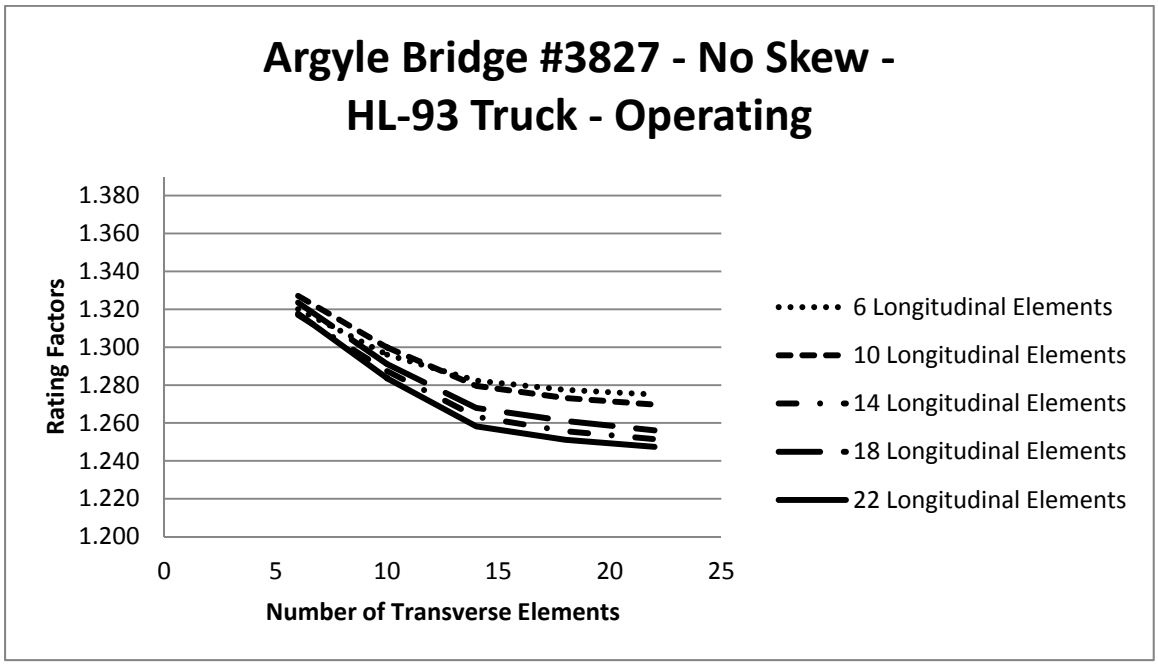

Figure 9 - Effects on Operating Rating Factor with an Increase in Mesh Elements under HL-93 Truck and Lane Load for Argyle Township Bridge #3827.

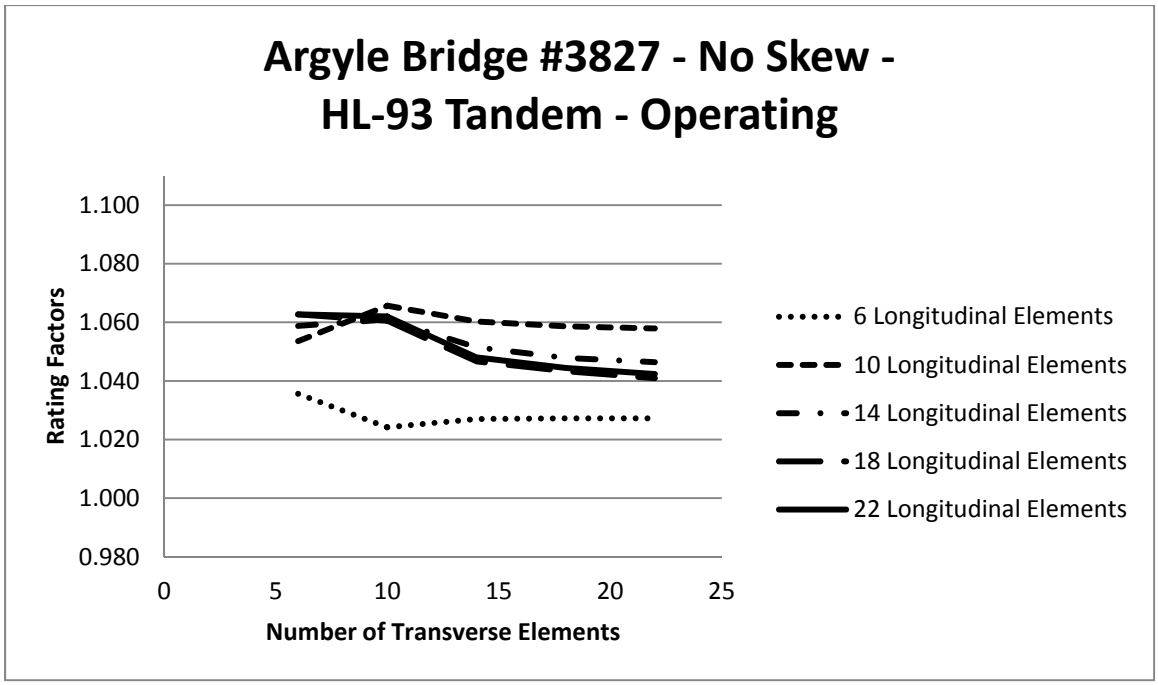

Figure 10- Effects on Operating Rating Factor with an Increase in Mesh Elements under HL-93 Tandem and Lane Load for Argyle Township Bridge #3827

3.3.1 Mesh Size Recommendation for Non-Skewed Bridges

From this study and more testing that was done using SlabRate it was found that the number of both longitudinal and transverse elements has an effect on live load moments and rating factors. For final results the mesh should consist of at least 14 longitudinal and 14 transverse elements. Fewer elements can be used for initial analyses to decrease the computational time and estimate an initial rating factor, but is not recommended to use those results for the final rating. For particularly long or wide bridges (structures with a large planar aspect ratio), the number of elements in either the longitudinal or transverse directions may need to be increased to maintain element aspect ratios less than or equal to three and ensure good element accuracy. Figure 11 and 12 below show the recommended mesh sizes for Levant Bridge #5253 and Argyle Township Bridge #3827.

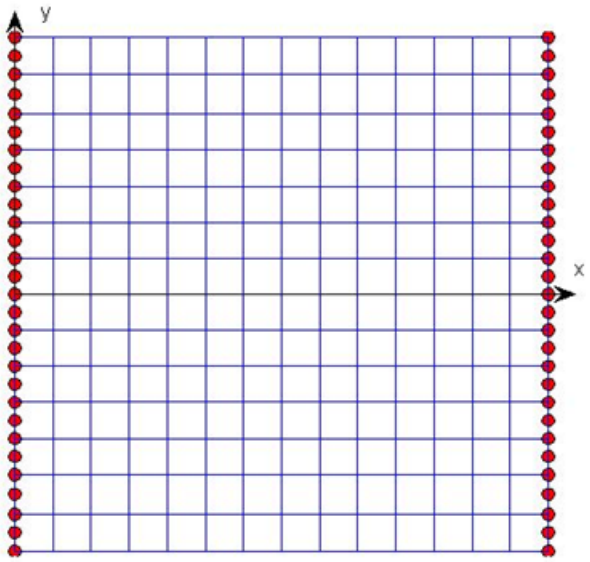

Figure 11 – Levant Bridge #5253 Recommended Finite Element Mesh, 14 Longitudinal Elements and 14 Transverse Elements.

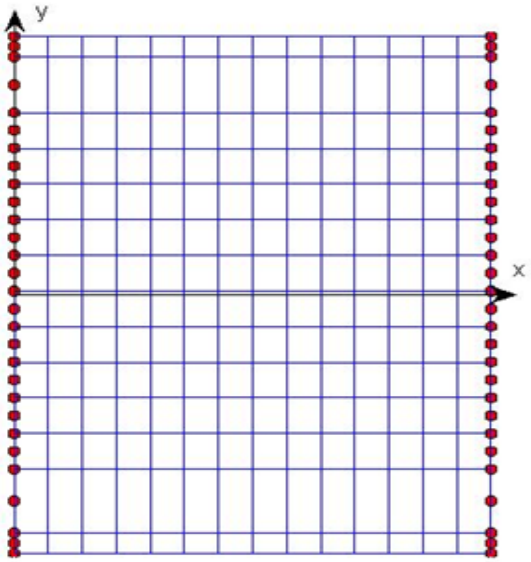

Figure 12 – Argyle Township Bridge #3827 Recommended Finite Element Mesh, 14 Longitudinal Elements and 14 Transverse Elements.

3.4 SlabRate Convergence for Skewed Bridges

Two different bridges, each with two separate skew angles, were analyzed to determine the required degree of mesh refinement in both the longitudinal and transverse direction for skewed bridges. The bridges that were analyzed were a modified Brewer Bridge #5638, at skew angles of 45° and 20°, and Carmel Bridge #5191, at skew angles of 45° and 30°.

3.4.1 Modified Brewer Bridge #5638

The Brewer Bridge span length is 7.042 m from centerline to centerline of the supports and the bridge width is 11.43 m. The slab thickness is 0.349 m, with reinforcing providing a moment resistance of 314.66 kN-m/m along with a wearing surface of 0.051 m. To keep the bridge symmetric for simplicity, the bridge curb widths were taken as 1.067 m, the smaller of the two curb widths of the actual bridge, with a curb height of 0.305 m. The edge of lane offset from the curb was taken as 0.610 m, and rail weights were not used for simplicity. An elastic modulus of 19640 MPa was used along with a Poisson's ratio of 0.19 and a unit weight of 2400 kg/m^3 was used for the concrete. Two separate skew angles were used, 45° and 20° (45° is the skew of the actual bridge).

Design Loads, HL-93 truck and tandem along with lane loads, were used in the analysis. The live load moments of the Brewer Bridge with a 45° for different mesh sizes are shown in Figures 13 – 14 for HL-93 truck and tandem loads.

The mesh sizes that were used are 14 to 20 longitudinal elements with an increment of 2 elements. A range of 10 to 52 transverse elements were also used in the study. The number of longitudinal and transverse elements was always taken as even so there is a node at the center of the bridge.

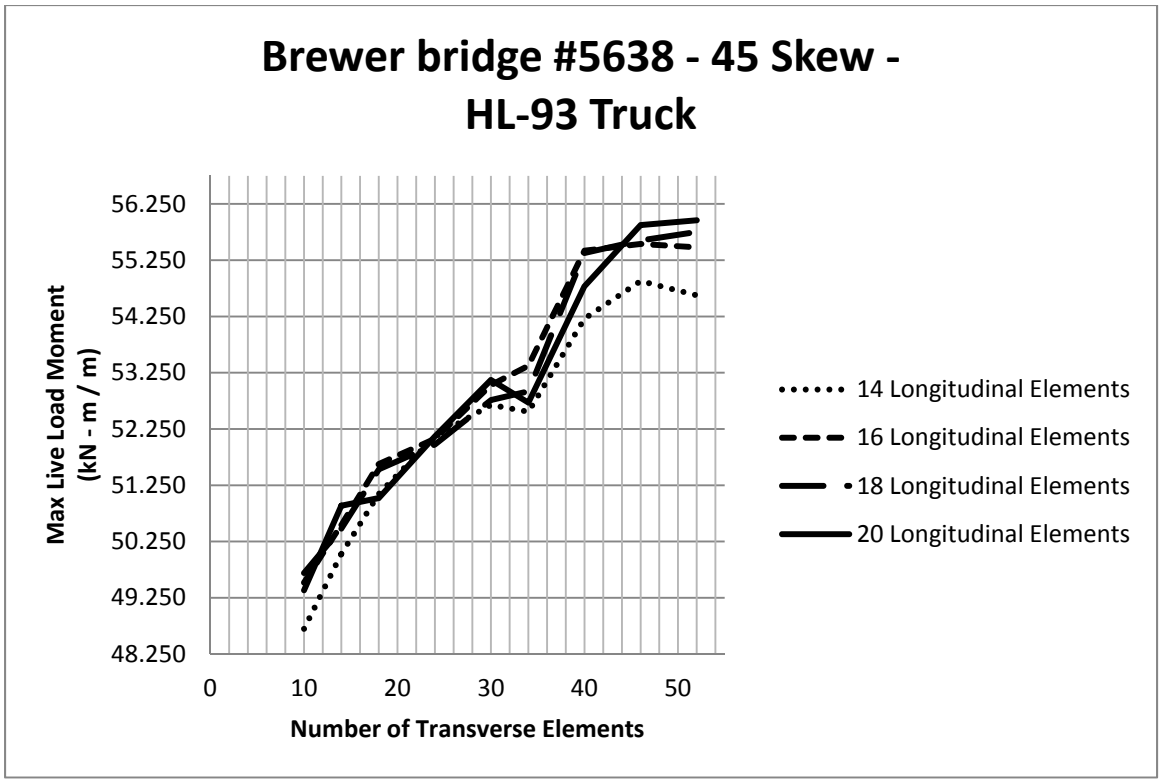

Figure 13 - Effects on Max Live load Moment with an Increase in Mesh Elements under HL-93 Truck and Lane Load for Brewer Bridge #5638, Skew of 45°

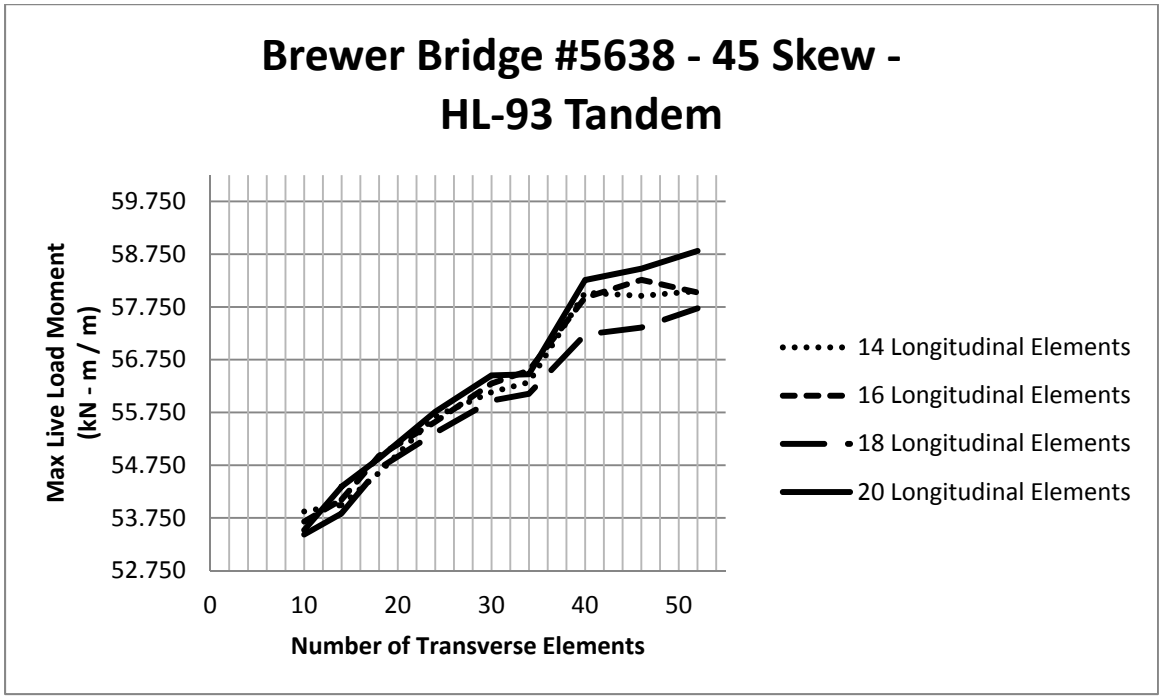

Figure 14 - Effects on Max Live Load Moment with an Increase in Mesh Elements under HL-93 Tandem and Lane Load for Brewer Bridge #5638, Skew of 45°

As the graphs show, the number of longitudinal elements has minimal affect on the maximum live load moment, an average of 1.4% and 0.6% increase from the smallest to the largest live load moment for HL-93 truck load and HL-93 tandem load respectively. The number of transverse elements has a much greater affect on the max live load moments. As seen from the graph the moment starts to converge to a relatively constant value at 40 transverse elements. The live load moment increases by an average of 11.4% for the HL-93 truck and 7.9% for the HL-93 tandem going from 10 to 40 transverse elements while only a 0.9% and 0.5% increase from 40 to 52 elements.

The Brewer Bridge was also analyzed with a skew angle of 20° while keeping all other aspects of the bridge the same. The results for the live load moments for different mesh sizes are shown below in Figures 15 and 16.

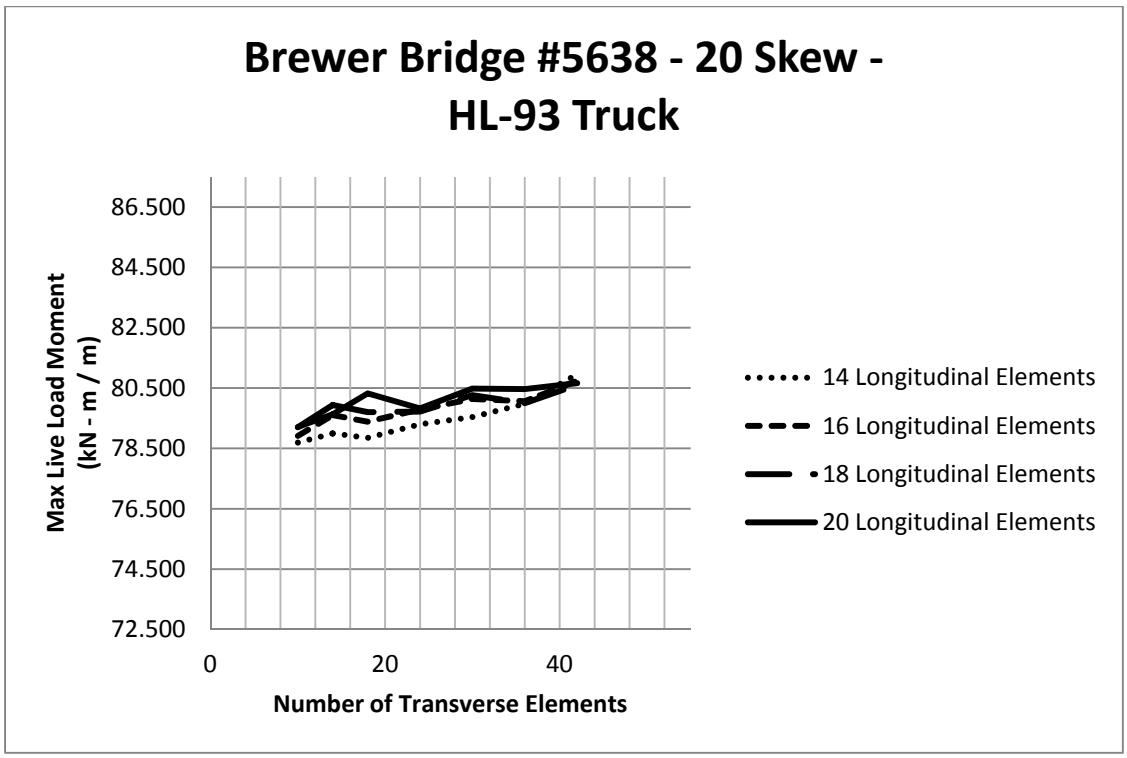

Figure 15 - Effects on Max Live load Moment with an Increase in Mesh Elements under HL-93 Truck and Lane Load for Brewer Bridge #5638, Skew of 20°

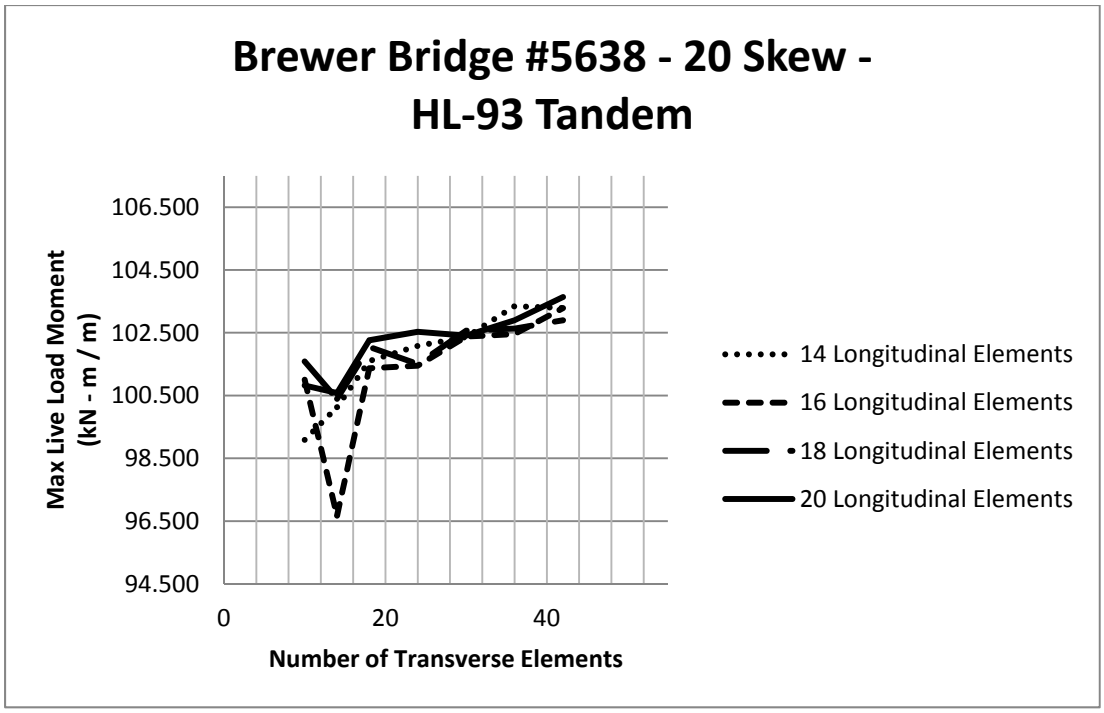

Figure 16 - Effects on Max Live load Moment with an Increase in Mesh Elements under HL-93 Tandem and Lane Load for Brewer Bridge #5638, Skew of 20°

With a decrease in a skew angle it was found that the effects of mesh refinement decreased significantly. The average percent increase in live load moment from 10 transverse elements to 42 transverse elements is 1.7% and 2.0% for HL-93 truck and HL-93 tandem respectively. Also the average percent increase from the smallest live load moment to the largest live load moment for the same number of transverse elements are 0.9% for HL-93 truck load and 1.5% for HL-93 tandem load. The 20° skew leads to the convergence of the moments with a smaller amount of elements in comparison to the 45° skew.

3.4.2 Carmel Bridge #5191

The Carmel Bridge span length is 10.16 m from centerline to centerline of the supports and a bridge width of 7.80 m. The slab thickness is 0.559 m deep, with reinforcing to provide a moment resistance of 468 kN–m/m with a wearing surface of 0.102 inches. The width of the bridge curbs were taken as 0.330 m, with a curb height of 0.305 m. The edge of lane offset from the curb was taken as 0.711 m for the top curb and 0.914 m for the bottom curb, and rail weights of 99.0 kN/m

were placed 0.133 m from each edge of the slab. An elastic modulus of 19640 MPa was used along with a Poisson's ratio of 0.19 and a unit weight of 2400 kg/m^3 was used for the concrete.

The same loads were applied to the Carmel Bridge as were applied to the Brewer Bridge (HL-93 truck load and a HL-93 tandem load). Both of these loads include the design lane live load. The live load moments for the actual Carmel Bridge with a skew of 30° are shown in Figures 17 – 18 for different mesh sizes.

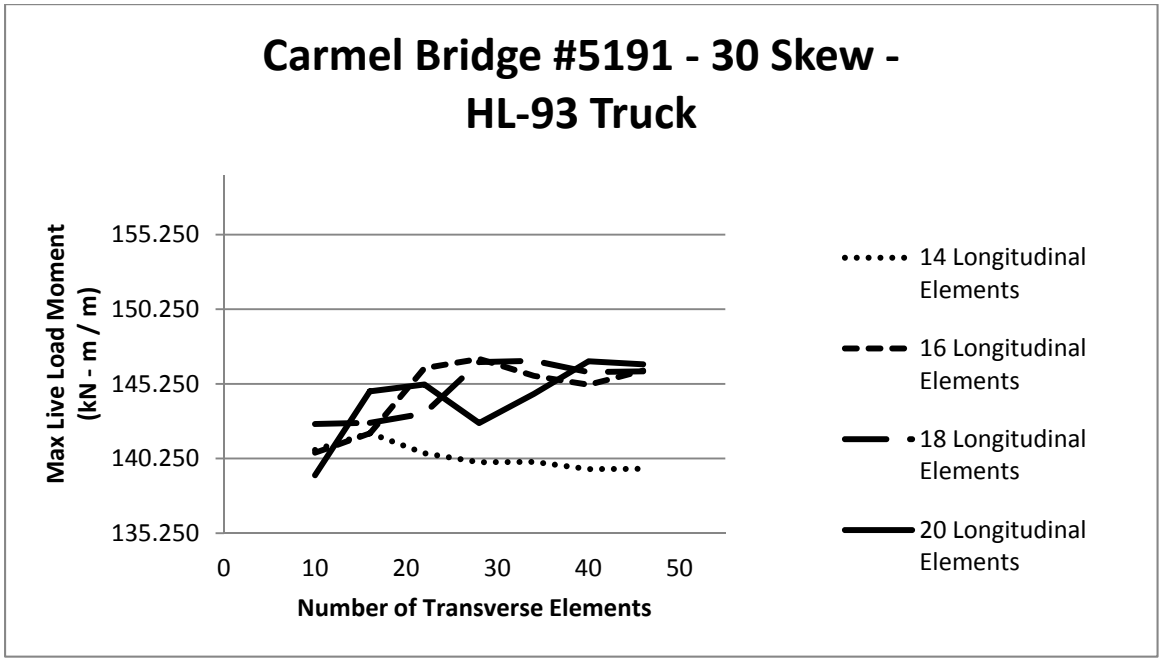

Figure 17 - Effects on Max Live load Moment with an Increase in Mesh Elements under HL-93 Truck and Lane Load for Carmel Bridge #5191, Skew of 30°

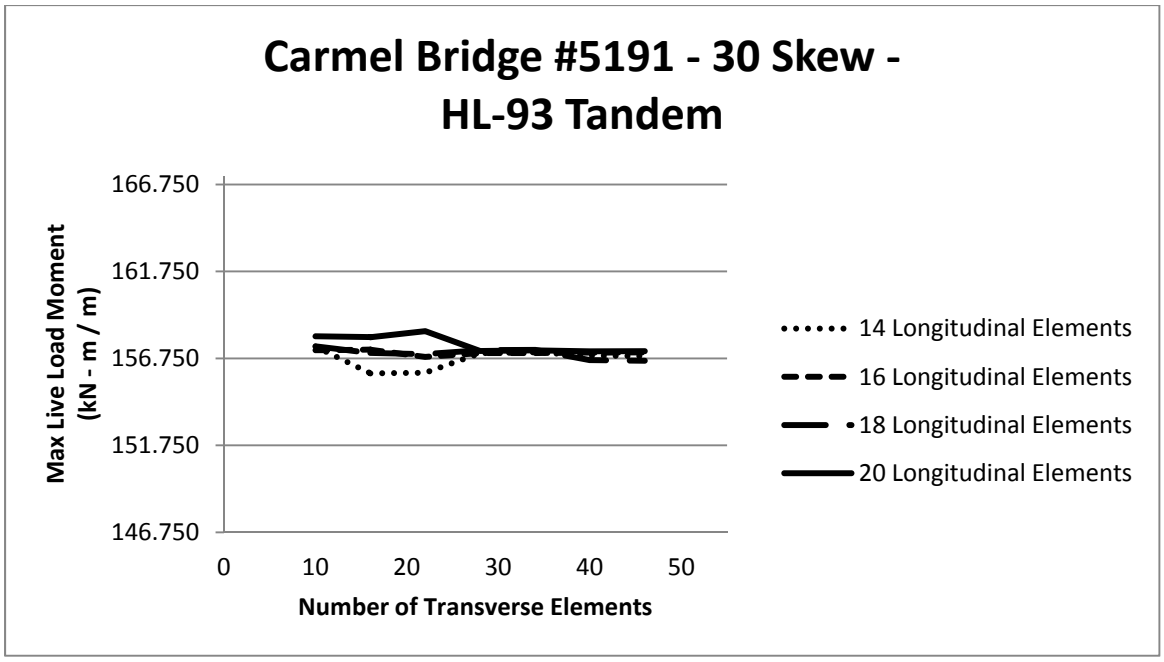

Figure 18 - Effects on Max Live load Moment with an Increase in Mesh Elements under HL-93 Tandem and Lane Load for Carmel Bridge #5191, Skew of 30°

Effects on the live load moment due to different size meshes for the Carmel Bridge #5191 with a 30° skew seem to be somewhat inconsistent. While looking at the 14 longitudinal elements for the HL-93 truck load, the live load moment decreases as more transverse elements are added, a 0.9% decrease from 10 transverse elements to 40 transverse elements. This does not follow the normal pattern of all the other bridges with different numbers of longitudinal elements; all others see an increase in live load moment while increasing the amount of transverse elements. The mesh configurations with 16, 18 and 20 longitudinal elements all follow the same pattern as all other bridges by increasing and converge to a relative maximum live load moment as more elements are added. The relative maximum live load for Carmel Bridge #5191 with a skew of 30° under HL-93 truck and lane load is 146.1 kN-m/m an average increase of 3.9% from 14 transverse to 40 transverse elements. The HL-93 tandem load seems to have already converged to a constant value by 10 transverse elements for all longitudinal mesh configurations, an average change of -0.2% from 10 to 40 transverse elements.

Carmel Bridge #5191 was also analyzed under a 45° skew while keeping all the other characteristics of the bridge the same. The results of the SlabRate live load moments with different mesh size are shown in Figures 19 and 20.

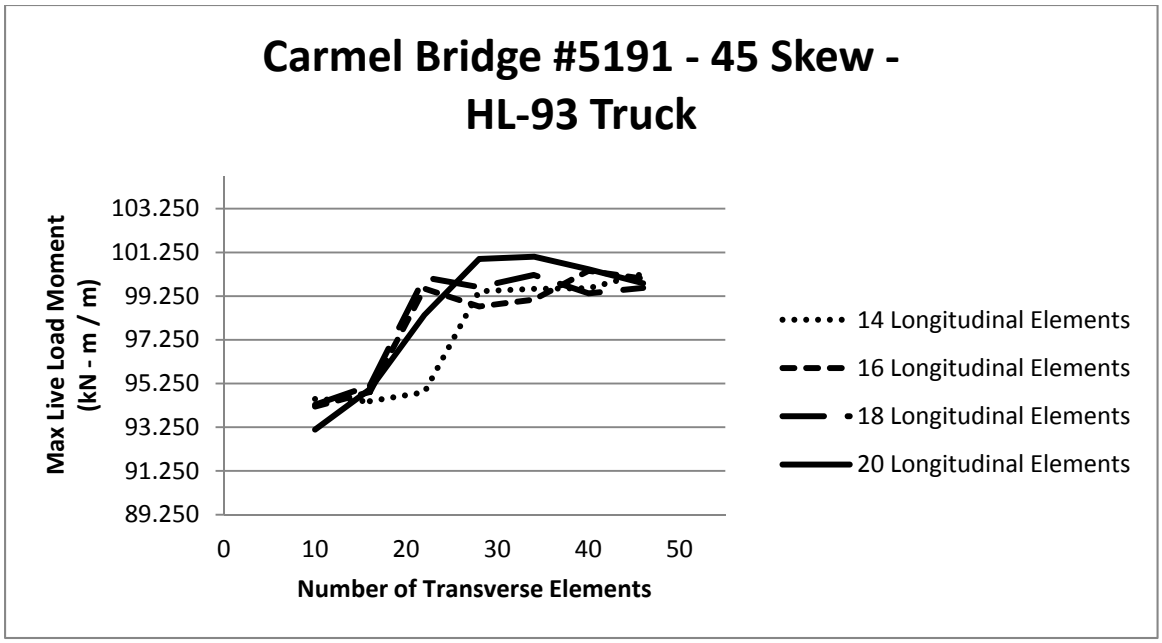

Figure 19 - Effects on Max Live Load Moment with an Increase in Mesh Elements under HL-93 Truck and Lane Loads for Carmel Bridge #5191, Skew of 45°

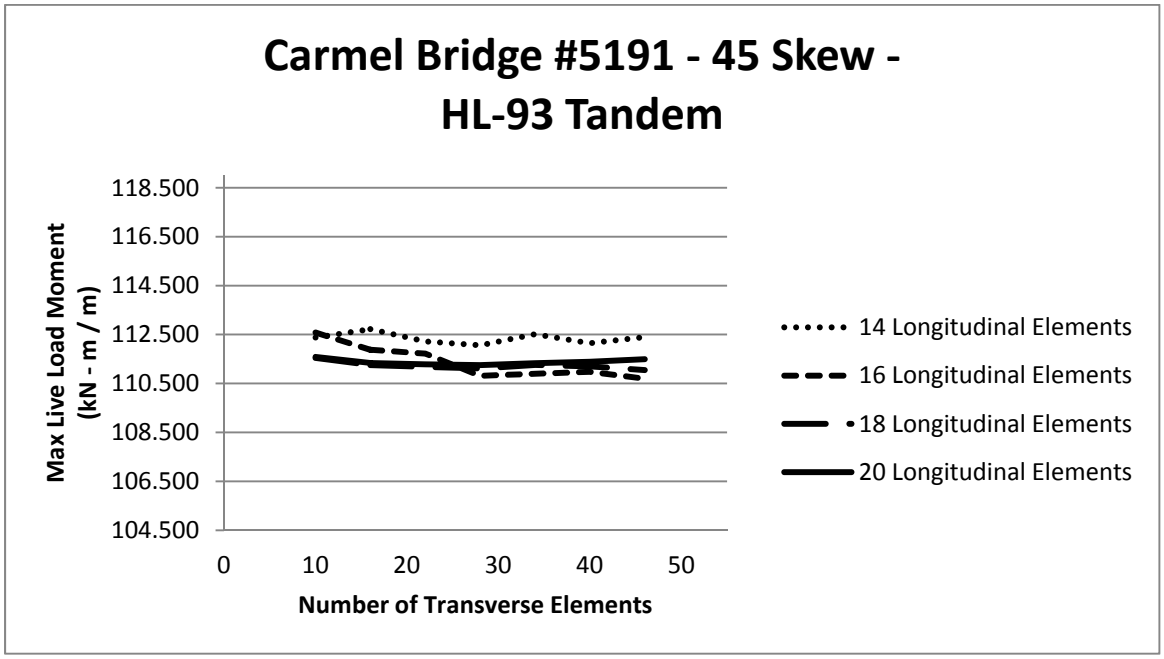

Figure 20 - Effects on Max Live Load Moment with an Increase in Mesh Elements under HL-93 Tandem and Lane Load for Carmel Bridge #5191, Skew of 45°

Carmel Bridge #5191 with a skew of 45° follows the same pattern as with a 30° skew. The HL-93 truck load requires more elements to converge to a relatively constant value than the HL-93 tandem load. The HL-93 truck converges at 28 transverse elements when 14 longitudinal elements are used and 22 transverse elements when more than 14 longitudinal elements are used. The HL-93 truck shows an average increase of 5.9% from 10 transverse elements until the number of transverse elements needed to converge to a relatively constant value, 28 transverse elements for 14 longitudinal elements and 22 transverse elements for 16, 18 and 20 longitudinal elements. After the values appear to converge to a relatively constant number an increase of 0.8% is seen from that point up to 46 mesh elements. These results indicate that the model converges to a constant value around 22 transverse elements. The 14 longitudinal meshes converged later but it might be closer to the 22 transverse elements if more mesh sizes were analyzed. The HL-93 tandem load does not show any increase in live load moment due to an increase in the number of elements. An average 0.6% change from 10 to 40 transverse elements shows that the HL-93 tandem load converges quickly.

3.4.3 Recommendation for Mesh Refinement of Skew Slab Bridges

When considering how skew affects the finite element analysis code SlabRate, it was found that the amount of transverse elements significantly affects the live load moments and thus the rating factors. All the results showed that the number of longitudinal elements had a lesser effect on the rating factors and moments. It was also found that with an increase of skew angle more transverse elements are needed to have the moments and rating factors converge to a constant value. Additionally, the width of the bridge also seems to have an effect on the live load moments and the rating factors. This is likely because the Brewer Bridge is 11.43 m wide while the Carmel Bridge is only 7.80 m wide, and the rating factors and live load moments for the Brewer Bridge took more transverse elements to converge, around 40 with a skew angle of 45°, while the Carmel Bridge with a skew angle of 45° only needed about 22 transverse elements to converge to a

constant value. Based on the analyses conducted here, the recommended mesh size is a minimum of 14 longitudinal and 40 transverse elements when there is a significant skew angle in the bridge. A mesh size of 14 longitudinal and 14 transverse elements can be used for a bridge width no skew.

Smaller skew angles may be accommodated with intermediate levels of mesh refinement. Figures 21 and 22 show the recommended finite element meshes for the Brewer bridge #5638 with a 45 degree skew and the Carmel bridge #5191 with a 30 degree skew, the actual skews of the bridges. Another factor that must be considered when constructing the mesh is the element aspect ratio, which in general must be kept to be less than 3:1. Particularly long or wide slab bridges may require more refined meshes than those used here to ensure that this aspect ratio is not exceeded.

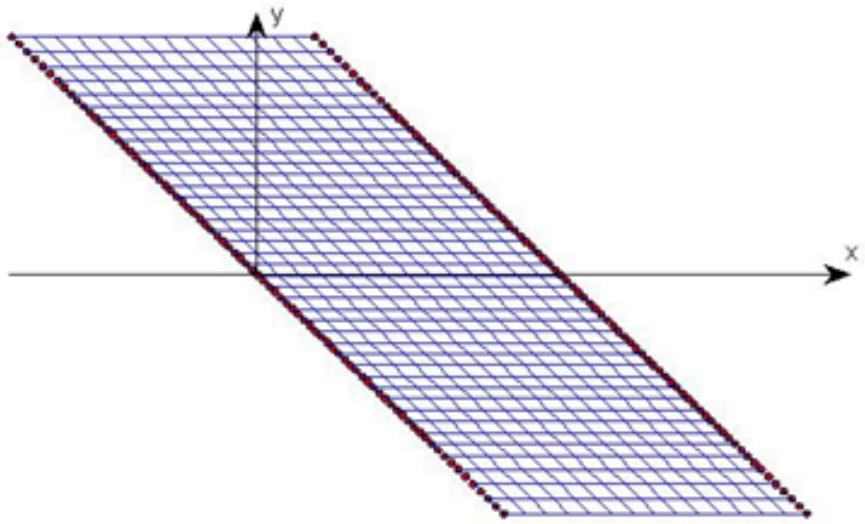

Figure 21 – Brewer Bridge #5638 Recommended Finite Element Mesh, 14 Longitudinal Elements and 40 Transverse Elements.

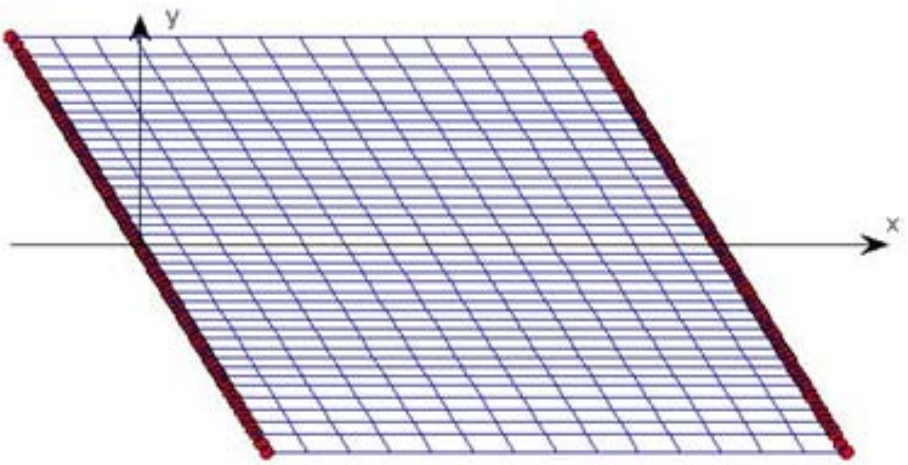

Figure 22 – Carmel Bridge #5191 Recommended Finite Element Mesh, 14 Longitudinal Elements and 40 Transverse Elements.

3.5 Comparison of SlabRate with Commercial FE Software

After SlabRate was developed, the solutions it created were verified using commercial software to ensure that the underlying finite-element code is correct. This was done by creating parallel models of identical bridges using both commercial finite element software and SlabRate and comparing the maximum moments and location of those moments due to a variety of live and dead loads. Two different commercial finite element programs were used ANSYS (ANSYS 2009) and Abaqus (Abaqus 2009). Convergence studies were done for each commercial finite element program, and the models were also checked against known analytical solutions to verify the solutions of the models.

The ANSYS (ANSYS 2009) models were used to validate that SlabRate provides accurate solutions given the modeling assumptions of linear elasticity, and small deformations. ANSYS was used for these models since they were easily created using input text files and straightforward to modify for different bridge characteristics and truck positions.

The other major assumption in SlabRate is that the supports are pinned. However, this is not strictly true, since the slab may lift of part of one or both supports under live loading, especially if one or both abutments are skewed. To assess the significance of slab lift-off, parallel models of identical bridges were created in Abaqus (Abaqus 2009) that had compression-only supports (i.e. allowed support lift-off). Abaqus software was used instead of ANSYS to examine support lift-off because there were features in Abaqus that facilitated straightforward modeling of the compression-only support, whereas this phenomenon proved to be more difficult to model in ANSYS.

Models for three separate bridges were created. These bridges were Brewer Bridge #5638, Carmel Bridge #5191 and Levant Bridge #5253. The characteristics for these bridges are shown below in Table 2. These bridges were chosen because they capture a wide range of bridge skews

(45°, 30° and 0° for the Brewer Bridge, Carmel Bridge and Levant Bridge, respectively), and these bridges were also used in the convergences studies conducted with SlabRate.

Table 4 - Bridge Model Characteristics

Bridge	Brewer #5638	Carmel #5191	Levant #5253
Span (Centerline to Centerline) (m)	7.04	10.16	8.12
Width (m)	11.43	7.77	7.82
Skew Angle	45	30	0
Slab Thickness (m)	0.349	0.559	0.470
Wearing Surface Thickness (m)	0.051	0.102	0.102
Moment Resistance (kN-m/m)	314.7	468.0	307.1
Rail Weight (kN / m) Top/ Bottom	1.889 1.889	1.959 1.959	0.898 0.898
Top Curb Width/ Height (m)	0.308 1.816	0.305 0.330	0.305 0.559
Bottom Curb Width/ Height (m)	0.610 0.965	0.305 0.330	0.305 0.559

3.5.1 Comparison with Results of ANSYS simulations

The models that were created in ANSYS were compared to the results of SlabRate's finite element models for each of the three bridges. Dead loads and live loads were compared separately. The ANSYS models use SHELL281 elements, which are 8-noded shell elements that use quadratic shape functions without reduced integration and also incorporate the effects caused by shear. These elements were chosen since they are the element in the ANSYS library most similar to the elements used in SlabRate.

First the dead load moments were compared. The results for both the ANSYS models and SlabRate for different combinations of dead loads are shown below in Tables 5 – 7. Figures 23 – 25 show the moment contour plots for both ANSYS and SlabRate when all the dead loads are applied to each of the bridges.

The live load moments were then compared, the live loads only included the truck load, they did not include lane loads or the dynamic impact factor. The results for both ANSYS and SlabRate are shown in Tables 8 – 10. The location of the truck is considered to be the top wheel of the middle axle for the HL-93 truck and the top wheel of the front axle for the HL-93 tandem loads. The truck direction is considered to be the direction that the truck is traveling. The origin of the bridges is taken as the geometric center of the bridge. The wheel that provided the maximum moment was centered over an element corner node to ensure that SlabRate provided the maximum moment. This was necessary because the 8-noded elements used by SlabRate capture a linear variation in moment over the element area, so maximum moments always occur at a corner node.

Table 5 – Max Moment due to Dead Load for ANSYS and SlabRate for Brewer Bridge #5638

Dead Load Applied	ANSYS Model (kN-m/m)	SlabRate (kN-m/m)	Percent Difference (%)
Slab	23.72	23.70	0.05
Slab and Curb	37.75	37.42	0.86
Slab, Curb and Rail	40.39	40.09	0.73
Slab, Curb, Rail and Wearing Surface	41.38	41.04	0.81

Table 6 - Max Moment due to Dead Load for ANSYS and SlabRate for Carmel Bridge #5191

Dead Load Applied	ANSYS Model (kN-m/m)	SlabRate (kN-m/m)	Percent Difference (%)
Slab	123.70	123.76	0.05
Slab and Curb	130.31	130.26	0.04
Slab, Curb and Rail	135.81	135.64	0.12
Slab, Curb, Rail and Wearing Surface	154.74	154.62	0.08

Table 7 - Max Moment due to Dead Load for ANSYS and SlabRate for Levant Bridge #5253

Dead Load Applied	ANSYS Model (kN-m/m)	SlabRate (kN-m/m)	Percent Difference (%)
Slab	93.79	94.10	0.33
Slab and Curb	104.08	104.33	0.24
Slab, Curb and Rail	106.40	106.63	0.22
Slab, Curb, Rail and	122.12	122.43	0.25

Wearing Surface			

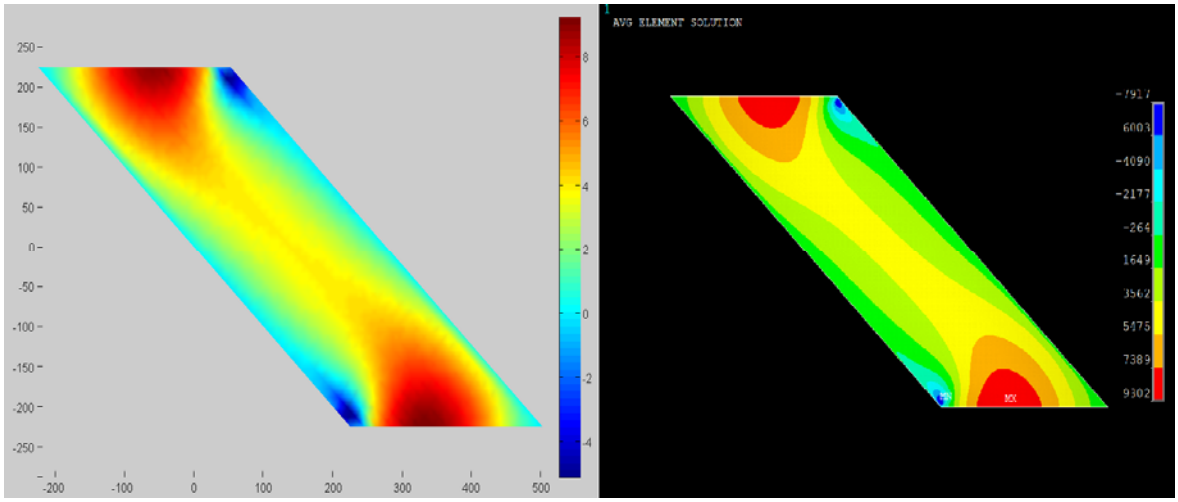

Figure 23 – Moment Contour Plots with all Dead Loads Applied for Brewer Bridge #5638

Left: SlabRate **Right**: ANSYS Model

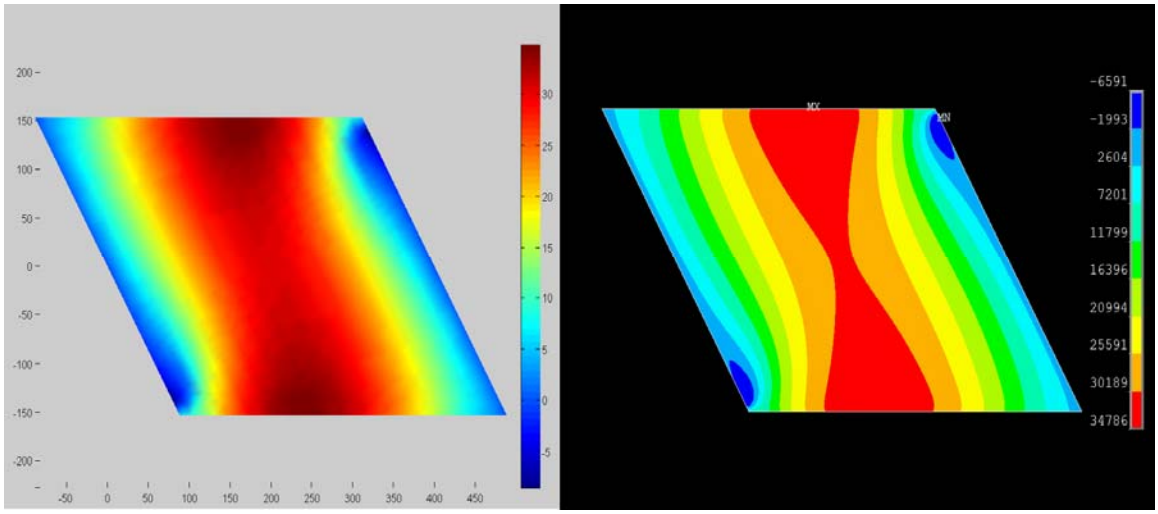

Figure 24 – Moment Contour Plots with all Dead Loads Applied for Carmel Bridge #5191

Left: SlabRate **Right**: ANSYS Model

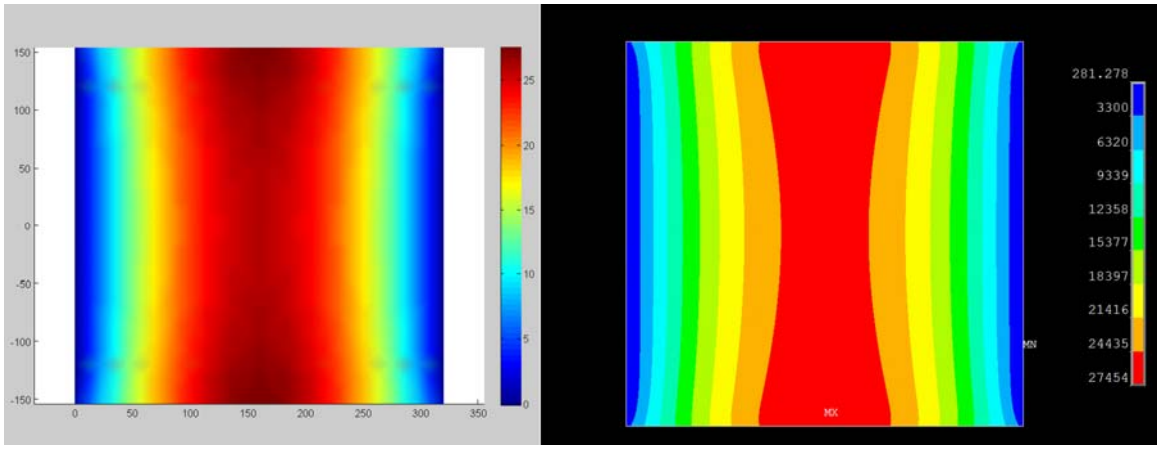

Figure 25 – Moment Contour Plots with all Dead Loads Applied for Levant Bridge #5253

Left: SlabRate **Right**: ANSYS Model

Table 8 - Max Moment due to Live Load for ANSYS and SlabRate for Brewer Bridge #5638

Truck Type	Location (cm)	Truck Direction	ANSYS Model (kN-m/m)	SlabRate (kN-m/m)	Percent Difference (%)
HL – 93 – Truck	(0,0)	Left	27.69	27.36	1.16
HL – 93 – Truck	(-442.13,341.53)	Left	26.48	26.13	1.31
HL – 93 – Tandem	(116.75,15.83)	Right	28.93	28.51	1.44

Table 9 - Max Moment due to Live Load for ANSYS and SlabRate for Carmel Bridge #5191

Truck Type	Location (cm)	Truck Direction	ANSYS Model (kN-m/m)	SlabRate (kN-m/m)	Percent Difference (%)
HL – 93 – Truck	(-17.6,155.4)	Right	53.73	53.04	1.28
HL – 93 – Truck	(292.10,233.17)	Right	60.39	59.77	1.04
HL – 93 – Tandem	(406.95,66.29)	Right	42.77	41.93	1.97

Table 10 - Max Moment due to Live Load for ANSYS and SlabRate for Levant Bridge #5253

Truck Type	Location (cm)	Truck Direction	ANSYS Model (kN-m/m)	SlabRate (kN-m/m)	Percent Difference (%)
HL – 93 – Truck	(0,223.5)	Right	53.60	53.24	0.66
HL – 93 – Truck	(310.8,111.8)	Right	52.05	51.58	0.91
HL – 93 – Tandem	(58.0,167.6)	Right	61.99	61.62	0.59

The results using SlabRate and ANSYS for both dead loads and live loads compare very well to each other. The maximum dead load moment percent differences range from 0.04% to 0.86%, while the maximum live load moment percent difference ranges from 0.01% to 1.97%. The average percent differences were 0.32% and 0.76% for dead load and live load models respectively. Along with the maximum values for dead load moments being within 1% the moment, contour plots for all dead loads are also very similar. This shows that the predicted moment values over the entire bridge are similar for both ANSYS and SlabRate at each point along the bridge. The live load moment contour plots from ANSYS and SlabRate which are not shown here also provide very similar shapes and magnitudes over the entire bridge.

3.5.2 Examination of Assumption of Pinned Supports

After the finite element program SlabRate was verified given the assumptions of linearly elasticity and small deformations using ANSYS, the significance of slab lift-off was examined using Abaqus. All of the Abaqus models used an S8R element, which is an 8-node doubly curved thick shell element with reduced integration. The S8R element is also a shear flexible element and uses quadratic shape functions, and is very similar to the element used by SlabRate.

To model slab lift-off, the abutments were modeled as solid concrete volumes meshed with bridge elements, and compression-only contact between the slab and each abutment was explicitly simulated. Because of this, the Abaqus models were nonlinear. Additionally, the

kinematics of the slab lift-off in the Abaqus models will provide a different maximum moment due to the change in the effective span length of the bridge from the centerline-support to centerline-support span assumed by SlabRate to face-of-support to face-of-support. Figure 26 shows a screen shot of a deformed model illustrating how the effective span becomes the clear span as the slab bends and bears only on the inside face of the abutment.

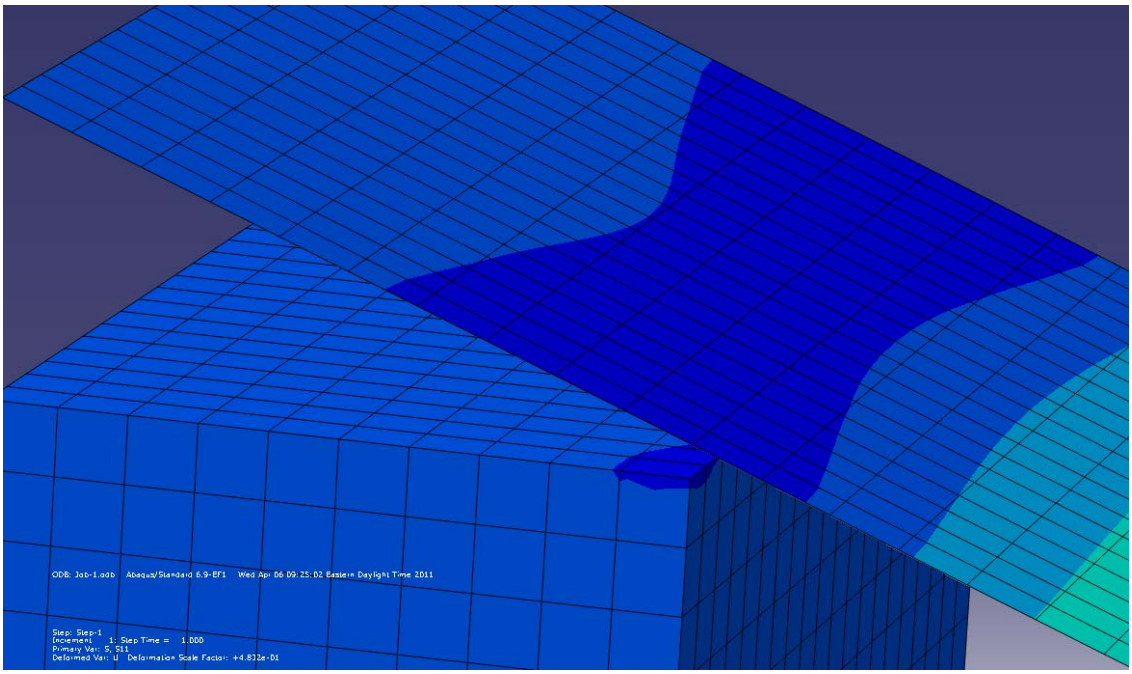

Figure 26 - Example of the Slab Lift Off from the Support and the How Effective Length Becomes the Clear Span

The ANSYS models, as discussed in the previous sections, used a linear analysis so the dead loads and live loads could be compared separately and the effects of both could be added using the principle of superposition. The loads applied to the Abaqus support lift-off models were factored since the analysis was non-linear. To isolate factored live loads effects, the Abaqus models were first analyzed under all factored dead and live loads, and then analyzed under only factored dead loads. The difference between the two separate loadings is the effect of the factored live loads.

The maximum factored live load moments predicted by the Abaqus models with compression-only supports are compared to the factored live load moments produced by SlabRate in Tables 11 – 12 for the Brewer and Levant Bridges respectively. These moments are located at the same location, the middle of a tire. Abaqus models were only created for Brewer Bridge #5638 and Levant Bridge #5253, as they are the both extremes in terms of skew angle, 45° and no skew respectively. The Abaqus models provided a somewhat lower maximum moment, due to the change in the effective span of the bridge as explained above.

Table 11 - Factored Max Live Load Moment due to Live Load for SlabRate and Abaqus Lift-Off Models for Brewer Bridge #5638

Truck Type	Location (cm)	Truck Direction	Abaqus Model (kN-m/m)	SlabRate (kN-m/m)	Percent Difference (%)
HL – 93 – Truck	(0,0)	Left	60.43	63.68	5.1
HL – 93 – Truck	(-442.13,341.53)	Left	56.08	60.82	8.0
HL – 93 – Tandem	(116.75,15.83)	Right	64.10	66.36	3.4

Table 12 - Factored Max Live Load Moment due to Live Load for SlabRate and Abaqus Lift-Off Models for Levant Bridge #5253

Truck Type	Location (cm)	Truck Direction	Abaqus Model (kN-m/m)	SlabRate (kN-m/m)	Percent Difference (%)
HL – 93 – Truck	(0,223.5)	Right	118.97	123.92	4.0
HL – 93 – Truck	(310.8,111.8)	Right	111.81	120.05	6.9
HL – 93 – Tandem	(58.0,167.6)	Right	140.02	143.42	2.4

The results from the Abaqus Models and SlabRate provide similar results, all within 8.0% of each other. The percent difference is predominantly caused by the effective span length change. The effective length of the bridge that is used in the Abaqus model (clear span) could not be used for all the loading cases above in SlabRate as if the span length changed in SlabRate the maximum

moment would not be applied to a node. If the maximum moment does not occur directly on a node SlabRate will underestimate the moment, it would instead linearly interpolate the moment between the closest nodes which would both be lower than the true maximum moment. SlabRate still provides results within a reasonable tolerance to the Abaqus models while always over predicting the moment when SlabRate uses center-line to center-line instead of clear span. Two of the loading cases above could be analyzed using the clear span in SlabRate without having to change anything else except the span length and still have the maximum moment applied to a node. The results from changing the length of the bridge are shown below in Table 13. These results from SlabRate use the same effective span length as the Abaqus model (clear span).

Table 13 – Factored Max Live Load Moment due to Live Load for SlabRate and Abaqus Lift-Off Models using the same Effective Span Length

Bridge	Truck Type	Location (cm)	Truck Direction	Abaqus Model (kN-m/m)	SlabRate (kN-m/m)	Percent Difference (%)
Brewer #5638	HL – 93 – Truck	(0,0)	Left	60.43	60.94	0.8
Levant #5253	HL – 93 – Truck	(0,223.5)	Right	118.97	118.71	0.2

With these two load cases provided very similar results as the Abaqus models for the same span length its shows that the major discrepancy between the Abaqus models and SlabRate's models are the change in effective span length. The reason why these loading cases could be used is because the maximum moments appeared at the center of the bridge where there was nodes. With changing the length of the bridge all the nodes along the *x*-direction will shift due to the fact you will have the same number of evenly spaced nodes. Nodes along the centerline will not shift as long as an even number of nodes are used so there are always nodes along the center of the bridge. The *y*-direction nodes will remain in the same position since the width of the bridges remains the same.

3.5.3 Conclusions of comparison of SlabRate with commercial FE software

The main objective of the modeling reported here was to ensure that the SlabRate finite-element implementation was correct for evaluating simply-supported and continuous flat slab bridges. The results from the ANSYS models and the SlabRate program compare very well to each other, indicating that SlabRate provides accurate solutions given the modeling assumptions of linear elasticity and small deformations.

The results from the Abaqus models that account for slab lift-off also compare well to the SlabRate program, with SlabRate giving conservative results in all cases. This conservatism may be explained by the change in effective span length captured by Abaqus due to slab lift-off.

4 Bridge Information

The characteristics of each of the twenty bridges that were load-rated using the conventional strip width method and the finite element program SlabRate are summarized in Tables 14 and 15. All the bridges were assumed to have an elastic modulus of 19640 MPa, along with a Poisson's ratio of 0.19 and a unit weight of concrete equal to 2400 kg/m^3. All the plans were provided by the MaineDoT and each bridge is located in Maine within a two hour travel time from the greater Bangor area.

Dimensions were verified by bridge visits conducted during July and August of 2010 and May 2011. The dimensions that were verified included slab thickness, curb width, curb height (both total height and heights above wearing surface), rail dimensions, striped lane offset from curb, number of lanes, span length, span width and skew angle. These measurements were taken to verify that the bridge plans represented the actual structure. If there was a difference between a

measured dimension and a dimension taken from the plans, the measured value was used in the rating.

In some cases, wearing surface thickness for six bridges could be field verified from the field visits in which case γ_{DW} was set to 1.25 instead of 1.50 per Table 6A.4.2.2-1 in AASHTO's Manual for Bridge Evaluation (AASHTO 2009). The six bridges for which the wearing surface was field verified were Argyle Township Bridge #3427, Bradford Bridge #3430, Carmel Bridge #5191, Levant Bridge #5253, Milford Bridge #2070 and Milo Bridge #2931. The wearing surface thicknesses of the other fourteen bridges could not be field verified, so the thicknesses in the plans were assumed to be correct and γ_{DW} was set to 1.50.

During the bridge visits, striped lane offset from the curb was measured. While analyzing bridges using SlabRate, wheel lines were placed no closer than 60.1 cm from the face of the curb, or at the striped lane edge.

The values for concrete compressive strength ($f_c^{'}$) and yield strength of the reinforcing steel (f_y) for each of the bridges are given in Tables 14 and 15. These values were assumed according to tables 6A.5.2.1-1 and 6A.5.2.2-1 of the *Manual for Bridge Evaluation* (AASHTO 2009) based on the year each bridge was constructed. Exceptions to this are the Albion Bridge #2529 and Milo Bridge #293 for which the value of f_y was specified in the plans.

All rail weights were modeled as constant distributed loads in the analysis. The maximum moments for each bridge caused by the actual field-measured rails were determined from measured dimensions and calculated weights assuming point loads where the posts are located. From these maximum moments, a constant distributed load was calculated produced the same maximum moment expected based on the actual post locations. The constant distributed load was used in the analysis since it was easier to apply in the finite element program SlabRate.

Both the Albion Bridge #2529 and Levant Bridge #5253 were two span structures. Neither of these bridges were continuous bridges, and therefore were modeled as a single span bridges with the larger of the two spans used in the analysis. The larger of the two spans were used since each span had the same thickness and reinforcing, and as thus the longest span would control since the dead and live load moments would be greater.

All condition factors were taken from the MaineDoT bridge inspections (MaineDoT 2008). All of the bridge inspections were performed by the MaineDoT between January 2008 and December 2009. Hermon Bridge #2205 was determined to have a condition factor (φ_c) equal to 0.95 (AASHTO 2009) i.e. structural condition of the bridge found to be fair. All the other bridges had a φ_c of 1.0 (AASHTO 2009), i.e. structural condition of the bridges found to be either good or satisfactory.

Table 14 - Summary of Bridge Characteristics

Bridge	Albion #2529	Argyle #3427	Bradford #3430	Brewer #5638	Carmel #5191	Carmel #5632	Chester #5907	Exeter #5838	Greenfield #5605	Hermon #2205
Length (m)	6.33	6.66	7.16	7.04	10.16	6.69	11.31	7.59	6.66	5.79
Width (m)	7.32	8.43	7.62	11.43	7.77	8.38	8.84	9.14	7.77	9.14
Skew Angle	43.87	0	0	45	30	30	0	10.25	20	0
Slab Thickness (m)	0.381	0.406	0.419	0.349	0.559	0.343	0.610	0.470	0.343	0.445
Wearing Surface Thickness (m)	0.013	0.076	0.076	0.051	0.102	0.076	0.102	0.522	0.330	0.127
f'_c (MPa)	17.24	17.24	17.24	17.24	17.24	17.24	20.68	20.68	17.24	17.24
f_y (MPa)	248.2	227.5	227.5	275.8	227.5	275.8	275.8	275.8	257.8	227.5
Moment Resistance (kN-m/m)	178.7	288.7	240.3	314.7	468.0	286.9	904.0	481.6	277.7	285.8
Rail Weight (kN / m) Top/ Bottom	1.236 1.392	2.222 2.222	1.582 1.582	1.889 1.889	1.959 1.959	5.039 5.039	4.343 4.343	0.327 0.327	2.358 2.358	0.192 0.192
Top Curb Width/ Height (m)	0.457 0.432	0.330 0.343	0.305 0.457	1.829 0.308	0.305 0.330	0.330 0.330	0.457 0.254	0.305 0.775	0.521 0.305	0.229 0.457
Bottom Curb Width/ Height (m)	0.457 0.432	0.330 0.343	0.305 0.457	1.067 0.290	0.305 0.330	0.330 0.330	0.457 0.305	0.305 0.521	0.521 0.305	0.229 0.457

Table 15 – Summary of Bridge Characteristics

Bridge	Levant #5253	Liberty #3493	Linneus #5311	Linneus #5773	Milford #2070	Milo #2931	Monroe #5538	Newcastle #5608	Palmyra #5699	Sherman #2899
Length (m)	8.12	7.85	6.62	7.54	8.34	7.47	8.77	8.15	6.57	9.21
Width (m)	7.82	7.62	8.33	9.14	9.25	11.58	8.41	8.99	9.14	10.29
Skew Angle	0	15	30	25	15	0	7.75	6	0	16.5
Slab Thickness (m)	0.470	0.457	0.394	0.356	0.419	0.457	0.432	0.394	0.330	0.533
Wearing Surface Thickness (m)	0.102	0.203	0.203	0.178	0.114	0.102	0.152	0.102	0.072	0.102
f'_c (kPa)	17.24	17.24	17.24	20.68	17.24	20.68	17.24	17.24	17.24	17.24
f_y (MPa)	227.5	227.5	227.5	275.8	275.8	413.7	275.8	275.8	275.8	227.5
Moment Resistance (kN-m/m)	307.1	291.5	249.4	329.8	451.9	642.5	502.6	404.0	264.5	409.7
Rail Weight (kN / m) Top/ Bottom	0.898 0.898	6.807 6.807	0.965 0.965	0.288 0.288	1.187 1.187	2.632 4.028	1.273 1.273	2.246 2.246	0.232 0.236	2.729 2.379
Top Curb Width/ Height (m)	0.305 0.559	0.330 0.381	0.508 0.279	0.305 0.305	0.305 0.359	0.279 2.235	0.546 0.356	0.521 0.254	0.254 0.318	1.829 0.305
Bottom Curb Width/ Height (m)	0.305 0.559	0.330 0.381	0.508 0.279	0.305 0.305	0.305 0.356	0.127 0.381	0.546 0.356	0.521 0.305	0.254 0.318	0.533 0.305

Photos of each bridge are shown in Figures 27 – 49. These photos show the real rails that were used to create the equivalent distributed loads. These photos also show the conditions of the roadways, curbs and rails. The dates of the bridge visits are also provided in the caption of each bridge photo.

Figure 27 – Photo of Albion Bridge #2529 from Bridge Visit in August 2010.

Figure 28 – Photo of the Rail on Albion Bridge #2529 from Bridge Visit in August 2010

Figure 29 - Photo of Argyle Bridge #3827 Rails from Bridge Visit Conducted July 2010

Figure 30 - Photo of Bradford Bridge #3430 Rail from Bridge Visit Conducted July 2010

Figure 31 - Photo of Brewer Bridge #5638 from Bridge Visit Conducted in July 2010

Figure 32 - Photo of Carmel Bridge #5191 Rail from Bridge Visit Conducted in July 2010

Figure 33 – Photo of Carmel Bridge #5632 from Bridge Visit Conducted in May 2011

Figure 34 – Photo of Chester Bridge #5907 from Bridge Visit Conducted May 2011

Figure 35 – Photo of Exeter Bridge #5838 from Bridge Visit Conducted in May 2011

Figure 36 – Photo of Greenfield TWP Bridge #5605 from Bridge Visit Conducted in May 2011

Figure 37 - Photo of Hermon Bridge Rail from bridge Visit Conducted August 2010.

Figure 38 - Photo of Levant Bridge #5253 from Bridge Visit Conducted in July 2010

Figure 39 - Photo of Levant Bridge #5253 Rail from Bridge Visit Conducted in July 2010

Figure 40- Photo of Liberty Bridge #3493 from Bridge Visit Conducted in May 2011

Figure 41 – Photo of Linneus Bridge #5311 from Bridge Visit Conducted in May 2011

Figure 42 – Photo of Linneus Bridge #5733 from Bridge Visit Conducted in May 2011

Figure 43 - Photo of Milford Bridge #2070 Rail from Bridge Visit Conducted July 2010

Figure 44 - Photo of Milo Bridge #2931 Top Rail from Bridge Visit Conducted August 2010

Figure 45 - Photo of Milo Bridge #2931 Bottom Rail from Bridge Visit Conducted August 2010

Figure 46 – Photo of Monroe Bridge #5538 from Bridge Visit Conducted in May 2011

Figure 47 – Photo of Newcastle Bridge #5608 from Bridge Visit Conducted in May 2011

Figure 48 - Photo of Palmyra Bridge #5699 Rail from Bridge Visit Conducted in August 2010

Figure 49 – Photo of Sherman Bridge #5311 from Bridge Visit Conducted in May 2011

5 Load Rating Results

All the rating factors for the conventional strip width method and the SlabRate finite element model are given in Tables 16 – 20. The maximum live loads moments computed using both the conventional strip width method and the finite element program SlabRate are shown in Tables 21 – 25. These live load moments include a dynamic impact factor of 33% and also include lane load effects for vehicles where a lane load was also included. Based on the convergence studies presented previously, the mesh sizes that were used were 14 longitudinal and 14 transverse elements for non-skewed bridges, and 14 longitudinal and 40 transverse elements for skewed bridges.

The trucks used in the analysis were the design trucks (HL-93 truck and tandem loads with lane load) for both inventory and operating levels, AASHTO legal trucks (Type 3, Type 3S2 and Type 3-3), specialized hauling vehicles (SU4, SU5, SU6 and SU7) and MaineDoT rating trucks (C1, C2, C3, C4, C5, C6, C7). Each bridge was analyzed for each truck even if the rating factors for the bridge exceeded one for HL-93 and legal trucks to provide as much information as possible regarding rating factors and live load moments for each bridge.

Table 16 – Rating Factors for the Conventional Strip Width and Finite Element Analysis for Albion Bridge #2529, Argyle Bridge #3427, Bradford Bridge #3430 and Brewer Bridge #5638.

	Albion Bridge #2529		Argyle Bridge #3827		Bradford Bridge #3430		Brewer Bridge #5638	
Live Load Truck	Strip Width	FEA	Strip Width	FEA	Strip Width	FEA	Strip Width	FEA
Design Truck - Lane - Inventory	0.365	1.100	0.799	0.979	0.469	0.567	0.721	2.804
Design Tandem - Lane - Inventory	0.293	0.992	0.637	0.804	0.372	0.451	0.573	2.714
Design Truck - Lane - Operating	0.473	1.427	1.036	1.269	0.608	0.735	0.935	3.635
Design Tandem - Lane - Operating	0.380	1.286	0.825	1.043	0.482	0.585	0.743	3.518
AASHTO Type 3 Truck	0.471	1.536	1.026	1.288	0.603	0.734	0.929	4.232
AASHTO Type 3S2 Truck	0.516	1.686	1.126	1.413	0.651	0.797	1.006	4.623
AASHTO Type 3-3	0.572	1.870	1.246	1.579	0.733	0.894	1.128	5.166
AASHTO-notional	0.408	1.455	0.873	1.100	0.497	0.603	0.771	4.046
AASHTO-SU4	0.454	1.580	0.987	1.240	0.576	0.708	0.889	4.367
AASHTO-SU5	0.430	1.528	0.929	1.166	0.536	0.660	0.828	4.226
AASHTO-SU6	0.408	1.465	0.873	1.100	0.500	0.616	0.775	4.134
AASHTO-SU7	0.408	1.452	0.873	1.100	0.497	0.604	0.771	4.088
MaineDoT C1	0.403	1.397	0.872	1.116	0.507	0.624	0.783	3.772
MaineDoT C2	0.403	1.453	0.872	1.103	0.507	0.624	0.783	3.983
MaineDoT C3	0.403	1.453	0.872	1.104	0.507	0.624	0.783	4.034
MaineDoT C4	0.434	1.430	0.918	1.161	0.521	0.648	0.811	3.825
MaineDoT C5	0.392	1.248	0.857	1.071	0.506	0.617	0.779	3.336
MaineDoT C6	0.300	1.052	0.650	0.816	0.379	0.469	0.586	2.953
MaineDoT C7	0.375	1.187	0.799	1.073	0.462	0.564	0.714	3.158
MaineDoT C8	0.574	1.703	1.232	1.533	0.716	0.879	1.111	4.464
MaineDoT C9	0.369	1.063	0.813	0.986	0.483	0.580	0.744	2.690

Table 17 – Rating Factors for Conventional Strip Width and Finite Element Analysis for Carmel Bridge #5191, Carmel Bridge #5632, Chester Bridge #5907 and Exeter Bridge #5838.

	Carmel Bridge #5191		Carmel Bridge #5632		Chester Bridge #5907		Exeter Bridge #5838	
Live Load Truck	Strip Width	FEA	Strip Width	FEA	Strip Width	FEA	Strip Width	FEA
Design Truck - Lane - Inventory	0.354	0.934	0.741	1.522	1.090	1.375	0.818	1.200
Design Tandem - Lane - Inventory	0.325	0.832	0.593	1.321	1.052	1.286	0.660	0.950
Design Truck - Lane - Operating	0.459	1.210	0.960	1.972	1.413	1.783	1.060	1.555
Design Tandem - Lane - Operating	0.421	1.078	0.769	1.522	1.364	1.668	0.856	1.232
AASHTO Type 3 Truck	0.515	1.352	0.957	2.107	1.624	2.048	1.078	1.542
AASHTO Type 3S2 Truck	0.537	1.407	1.049	2.278	1.733	2.155	1.137	1.659
AASHTO Type 3-3	0.634	1.661	1.162	2.553	1.977	2.480	1.309	1.864
AASHTO-notional	0.380	1.004	0.812	1.857	1.195	1.465	0.862	1.279
AASHTO-SU4	0.486	1.281	0.918	2.099	1.554	1.942	1.025	1.496
AASHTO-SU5	0.462	1.208	0.862	1.991	1.464	1.832	0.948	1.409
AASHTO-SU6	0.418	1.093	0.812	1.896	1.336	1.663	0.878	1.297
AASHTO-SU7	0.396	1.034	0.812	1.866	1.263	1.550	0.862	1.282
MaineDoT C1	0.446	1.159	0.811	1.887	1.454	1.799	0.900	1.355
MaineDoT C2	0.388	1.019	0.811	1.888	1.224	1.493	0.878	1.282
MaineDoT C3	0.414	1.086	0.811	1.886	1.285	1.586	0.900	1.338
MaineDoT C4	0.432	1.102	0.858	1.949	1.330	1.657	0.910	1.340
MaineDoT C5	0.438	1.121	0.801	1.753	1.356	1.685	0.908	1.286
MaineDoT C6	0.326	0.841	0.604	1.375	1.041	1.291	0.677	0.933
MaineDoT C7	0.395	1.042	0.746	1.637	1.281	1.585	0.815	1.181
MaineDoT C8	0.621	1.571	1.155	2.397	2.020	2.505	1.273	1.816
MaineDoT C9	0.372	0.979	0.755	1.494	1.152	1.453	0.845	1.225

Table 18 – Rating Factors for Conventional Strip Width and Finite Element Analysis for Greenfield Bridge #5605, Hermon Bridge #2205, Levant Bridge #5253 and Liberty Bridge #5638.

	Greenfield Bridge #5605		Hermon Bridge #2205		Levant Bridge #5253		Liberty Bridge #5638	
Live Load Truck	Strip Width	FEA	Strip Width	FEA	Strip Width	FEA	Strip Width	FEA
Design Truck - Lane - Inventory	0.587	0.996	0.347	0.461	0.464	0.571	0.326	0.546
Design Tandem - Lane - Inventory	0.470	0.813	0.285	0.399	0.385	0.456	0.268	0.416
Design Truck - Lane - Operating	0.760	1.291	0.450	0.597	0.602	0.740	0.423	0.708
Design Tandem - Lane - Operating	0.609	1.053	0.369	0.518	0.499	0.591	0.347	0.539
AASHTO Type 3 Truck	0.758	1.299	0.454	0.633	0.632	0.751	0.438	0.682
AASHTO Type 3S2 Truck	0.831	1.418	0.497	0.688	0.657	0.757	0.459	0.733
AASHTO Type 3-3	0.920	1.577	0.551	0.764	0.767	0.913	0.532	0.828
AASHTO-notional	0.644	1.131	0.408	0.571	0.492	0.582	0.345	0.534
AASHTO-SU4	0.727	1.278	0.441	0.614	0.600	0.723	0.417	0.658
AASHTO-SU5	0.683	1.213	0.424	0.593	0.551	0.663	0.384	0.607
AASHTO-SU6	0.644	1.140	0.408	0.572	0.508	0.606	0.354	0.554
AASHTO-SU7	0.644	1.131	0.408	0.572	0.495	0.582	0.346	0.534
MaineDoT C1	0.643	1.142	0.394	0.573	0.514	0.629	0.365	0.572
MaineDoT C2	0.643	1.140	0.394	0.559	0.485	0.595	0.350	0.551
MaineDoT C3	0.643	1.140	0.394	0.556	0.514	0.628	0.365	0.571
MaineDoT C4	0.680	1.184	0.440	0.603	0.510	0.640	0.364	0.592
MaineDoT C5	0.634	1.080	0.377	0.515	0.517	0.635	0.369	0.581
MaineDoT C6	0.479	0.849	0.290	0.404	0.382	0.473	0.272	0.433
MaineDoT C7	0.592	1.015	0.360	0.493	0.464	0.566	0.331	0.533
MaineDoT C8	0.915	1.553	0.565	0.755	0.725	0.898	0.512	0.833
MaineDoT C9	0.598	0.999	0.347	0.455	0.467	0.588	0.338	0.564

Table 19 – Rating Factors for Conventional Strip Width and Finite Element Analysis for Linneus Bridge #5311, Linneus Bridge #5773, Milford Bridge #2070 and Milo Bridge #2931.

	Linneus Bridge #5311		Linneus Bridge #5773		Milford Bridge #2070		Milo Bridge #2931	
Live Load Truck	Strip Width	FEA	Strip Width	FEA	Strip Width	FEA	Strip Width	FEA
Design Truck - Lane - Inventory	0.502	1.184	0.679	1.285	0.906	1.260	1.975	2.361
Design Tandem - Lane - Inventory	0.403	1.057	0.547	1.062	0.767	1.038	1.575	1.909
Design Truck - Lane - Operating	0.651	1.535	0.880	1.666	1.175	1.634	2.560	3.061
Design Tandem - Lane - Operating	0.523	1.370	0.710	1.376	0.994	1.346	2.042	2.475
AASHTO Type 3 Truck	0.649	1.658	0.893	1.724	1.265	1.706	2.567	3.092
AASHTO Type 3S2 Truck	0.712	1.817	0.946	1.859	1.301	1.777	2.717	3.307
AASHTO Type 3-3	0.789	2.049	1.084	2.094	1.537	2.072	3.117	3.781
AASHTO-notional	0.553	1.497	0.717	1.413	0.960	1.324	2.070	2.556
AASHTO-SU4	0.623	1.662	0.851	1.683	1.194	1.649	2.441	2.975
AASHTO-SU5	0.586	1.582	0.788	1.572	1.094	1.515	2.257	2.801
AASHTO-SU6	0.553	1.513	0.730	1.451	1.005	1.388	2.097	2.578
AASHTO-SU7	0.553	1.498	0.717	1.420	0.974	1.331	2.070	2.560
MaineDoT C1	0.551	1.499	0.747	1.480	1.045	1.440	2.143	2.644
MaineDoT C2	0.551	1.494	0.730	1.446	0.974	1.351	2.103	2.571
MaineDoT C3	0.551	1.495	0.747	1.477	1.045	1.438	2.143	2.644
MaineDoT C4	0.584	1.531	0.755	1.494	1.025	1.425	2.173	2.690
MaineDoT C5	0.543	1.354	0.751	1.420	1.047	1.427	2.153	2.575
MaineDoT C6	0.410	1.088	0.562	1.106	0.759	1.073	1.606	1.961
MaineDoT C7	0.508	1.306	0.679	1.320	0.938	1.282	1.943	2.351
MaineDoT C8	0.784	1.853	1.052	1.974	1.465	1.964	3.027	3.580
MaineDoT C9	0.511	1.162	0.702	1.286	0.938	1.285	2.042	2.410

Table 20 – Rating Factors for Conventional Strip Width and Finite Element Analysis for Monroe Bridge #5538, Newcastle Bridge #5608, Palmyra Bridge #5699 and Sherman Bridge #2899.

	Monroe Bridge #5538		Newcastle Bridge #5608		Palmyra Bridge #5699		Sherman Bridge #2899	
Live Load Truck	Strip Width	FEA	Strip Width	FEA	Strip Width	FEA	Strip Width	FEA
Design Truck - Lane - Inventory	0.849	1.144	0.814	1.089	0.815	0.941	0.283	0.520
Design Tandem - Lane - Inventory	0.736	0.980	0.683	0.911	0.654	0.769	0.250	0.435
Design Truck - Lane - Operating	1.101	1.483	1.055	1.411	1.056	1.219	0.366	0.675
Design Tandem - Lane - Operating	0.955	1.271	0.855	1.181	0.848	0.996	0.324	0.564
AASHTO Type 3 Truck	1.221	1.613	1.123	1.483	1.053	1.237	0.408	0.723
AASHTO Type 3S2 Truck	1.235	1.639	1.164	1.544	1.155	1.357	0.418	0.740
AASHTO Type 3-3	1.483	1.958	1.364	1.808	1.279	1.509	0.506	0.879
AASHTO-notional	0.902	1.212	0.864	1.157	0.898	1.070	0.301	0.538
AASHTO-SU4	1.133	1.515	1.066	1.421	1.011	1.198	0.380	0.681
AASHTO-SU5	1.047	1.402	0.977	1.299	0.952	1.132	0.355	0.632
AASHTO-SU6	0.959	1.286	0.899	1.204	0.898	1.069	0.324	0.576
AASHTO-SU7	0.923	1.230	0.873	1.171	0.898	1.073	0.310	0.547
MaineDoT C1	1.004	1.351	0.932	1.253	0.896	1.074	0.341	0.605
MaineDoT C2	0.918	1.227	0.880	1.163	0.896	1.069	0.306	0.548
MaineDoT C3	1.004	1.329	0.932	1.250	0.896	1.069	0.333	0.594
MaineDoT C4	0.976	1.295	0.920	1.223	0.961	1.121	0.327	0.588
MaineDoT C5	1.002	1.321	0.935	1.226	0.881	1.031	0.339	0.593
MaineDoT C6	0.737	0.988	0.691	0.928	0.667	0.790	0.249	0.443
MaineDoT C7	0.898	1.189	0.840	1.105	0.824	0.976	0.304	0.542
MaineDoT C8	1.408	1.830	1.316	1.698	1.268	1.480	0.477	0.850
MaineDoT C9	0.884	1.172	0.844	1.112	0.829	0.948	0.295	0.545

Table 21 – Live Load Moments (kN – m/m) for Conventional Strip Width and Finite Element Analysis for Albion Bridge #2529, Argyle Bridge #3427, Bradford Bridge #3430 and Brewer Bridge #5638.

	Albion Bridge #2529		Argyle Bridge #3827		Bradford Bridge #3430		Brewer Bridge #5638	
Live Load Truck	Strip Width	FEA	Strip Width	FEA	Strip Width	FEA	Strip Width	FEA
Design Truck - Lane - Inventory	144.14	65.55	120.44	100.81	132.08	111.84	152.32	51.38
Design Tandem - Lane - Inventory	179.61	69.22	151.18	119.71	166.61	136.22	191.68	52.64
Design Truck - Lane - Operating	144.14	65.55	120.44	100.81	132.08	111.84	152.32	51.38
Design Tandem - Lane - Operating	179.61	69.22	151.18	119.71	166.61	136.22	191.68	52.64
AASHTO Type 3 Truck	108.81	45.04	91.18	72.67	99.81	81.43	115.01	32.82
AASHTO Type 3S2 Truck	99.21	41.02	83.13	66.28	92.51	66.90	106.21	27.12
AASHTO Type 3-3	89.61	37.51	75.09	59.31	82.20	77.31	94.72	30.30
AASHTO-notional	141.14	53.49	120.60	95.81	136.43	111.49	155.79	38.95
AASHTO-SU4	128.35	49.58	106.69	84.93	117.63	97.88	135.22	36.08
AASHTO-SU5	133.94	50.94	113.37	90.36	126.50	105.04	145.10	37.29
AASHTO-SU6	141.14	53.13	120.60	95.77	135.51	109.27	155.15	38.14
AASHTO-SU7	141.14	53.61	120.60	95.76	136.43	111.43	155.79	38.54
MaineDoT C1	142.81	69.83	120.71	94.36	133.62	107.66	153.45	42.44
MaineDoT C2	142.81	51.67	120.71	95.53	133.62	107.71	153.45	39.57
MaineDoT C3	142.81	51.70	120.71	95.42	133.62	107.72	153.45	39.07
MaineDoT C4	132.76	55.18	114.68	91.75	130.04	108.95	148.12	42.62
MaineDoT C5	146.82	63.21	122.80	98.35	133.98	112.30	154.25	47.24
MaineDoT C6	192.05	75.01	161.91	129.06	178.65	147.84	205.17	53.36
MaineDoT C7	153.58	66.49	131.69	104.56	146.67	122.80	168.25	49.91
MaineDoT C8	100.33	46.34	85.42	69.48	94.56	80.41	108.19	35.30
MaineDoT C9	155.98	74.21	129.50	109.42	140.31	119.57	161.49	58.58

Table 22 – Live Load Moments (kN – m/m) for Conventional Strip Width and Finite Element Analysis for Carmel Bridge #5191, Carmel Bridge #5632, Chester Bridge #5907 and Exeter Bridge #5838.

	Carmel Bridge #5191		Carmel Bridge #5632		Chester Bridge #5907		Exeter Bridge #5838	
Live Load Truck	Strip Width	FEA	Strip Width	FEA	Strip Width	FEA	Strip Width	FEA
Design Truck - Lane - Inventory	248.16	139.54	134.26	74.97	259.89	206.40	139.59	107.97
Design Tandem - Lane - Inventory	270.37	156.92	167.62	86.98	269.21	217.28	172.80	134.10
Design Truck - Lane - Operating	248.16	139.54	134.26	74.97	259.89	206.40	139.59	107.97
Design Tandem - Lane - Operating	270.37	156.92	167.62	86.98	269.21	217.28	172.80	134.10
AASHTO Type 3 Truck	165.89	93.67	101.06	53.03	169.57	134.75	102.89	80.34
AASHTO Type 3S2 Truck	159.26	76.38	92.12	49.05	158.89	126.10	97.55	73.28
AASHTO Type 3-3	134.84	90.01	83.23	43.77	139.32	113.07	84.74	66.45
AASHTO-notional	253.00	141.87	134.02	67.67	259.24	208.71	144.79	108.97
AASHTO-SU4	197.69	111.41	118.50	59.52	199.37	159.83	121.84	93.19
AASHTO-SU5	208.24	117.97	126.24	62.68	211.60	166.87	131.76	97.01
AASHTO-SU6	229.80	130.62	134.02	63.10	231.97	183.79	142.21	105.39
AASHTO-SU7	242.60	137.99	134.02	64.09	245.27	197.26	144.79	108.72
MaineDoT C1	215.48	122.97	134.11	63.40	213.03	169.91	138.74	102.86
MaineDoT C2	247.76	139.80	134.11	63.70	253.19	204.75	142.25	106.69
MaineDoT C3	232.12	131.41	134.11	63.41	241.23	192.71	138.74	102.22
MaineDoT C4	222.70	129.26	126.86	64.46	232.91	184.54	137.14	102.03
MaineDoT C5	219.28	127.14	135.80	71.72	228.42	184.27	137.49	108.34
MaineDoT C6	295.11	169.45	180.06	90.73	297.72	236.80	184.29	137.66
MaineDoT C7	243.49	138.19	145.77	76.21	241.89	195.87	153.11	115.77
MaineDoT C8	154.81	93.41	94.17	52.41	153.37	123.94	98.08	75.94
MaineDoT C9	258.65	145.48	144.08	83.49	268.85	217.09	147.64	115.91

Table 23 – Live Load Moments (kN – m/m) for Conventional Strip Width and Finite Element Analysis for Greenfield Bridge #5605, Hermon Bridge #2205, Levant Bridge #5253 and Liberty Bridge #3493.

	Greenfield Bridge #5605		Hermon Bridge #2205		Levant Bridge #5253		Liberty Bridge #5638	
Live Load Truck	Strip Width	FEA	Strip Width	FEA	Strip Width	FEA	Strip Width	FEA
Design Truck - Lane - Inventory	127.77	89.18	104.18	88.35	155.11	130.79	153.94	111.29
Design Tandem - Lane - Inventory	159.44	109.23	127.03	102.00	187.04	154.53	187.80	133.30
Design Truck - Lane - Operating	127.77	89.18	104.18	88.35	155.11	130.79	153.94	111.29
Design Tandem - Lane - Operating	159.44	109.23	127.03	102.00	187.04	154.53	187.80	133.30
AASHTO Type 3 Truck	96.17	66.44	77.53	62.55	110.82	91.26	111.47	79.01
AASHTO Type 3S2 Truck	87.67	60.86	70.69	57.55	106.53	75.11	106.45	73.47
AASHTO Type 3-3	79.18	54.72	63.84	51.80	91.26	90.09	91.81	65.05
AASHTO-notional	127.35	82.50	96.86	78.02	160.08	132.46	159.20	113.51
AASHTO-SU4	112.76	75.99	89.69	72.60	131.32	110.38	131.89	92.13
AASHTO-SU5	120.01	80.07	93.26	75.15	142.91	116.24	143.14	99.71
AASHTO-SU6	127.35	81.80	96.86	77.85	155.01	127.29	155.20	109.36
AASHTO-SU7	127.35	82.50	96.86	77.90	159.09	132.43	158.80	113.35
MaineDoT C1	127.53	81.92	100.45	77.72	153.31	122.51	150.44	105.96
MaineDoT C2	127.53	81.92	100.45	79.61	162.42	129.56	157.11	109.94
MaineDoT C3	127.53	81.92	100.45	80.10	153.31	122.74	150.44	106.05
MaineDoT C4	120.55	82.00	89.97	73.87	154.60	120.42	151.02	102.37
MaineDoT C5	129.31	89.86	105.03	86.42	152.29	121.40	149.10	104.26
MaineDoT C6	171.30	114.41	136.25	110.22	206.14	168.83	201.77	139.99
MaineDoT C7	138.56	95.58	109.80	90.36	169.88	140.99	166.23	125.58
MaineDoT C8	89.63	62.52	69.95	59.03	108.72	90.90	107.25	81.07
MaineDoT C9	137.18	97.20	113.95	97.84	168.52	138.78	162.58	119.70

Table 24 – Live Load Moments (kN – m/m) for Conventional Strip Width and Finite Element Analysis for Linneus Bridge #5311, Linneus Bridge #5773, Milford Bridge #2070 and Milo Bridge #2931.

	Linneus Bridge #5311		Linneus Bridge #5773		Milford Bridge #2070		Milo Bridge #2931	
Live Load Truck	Strip Width	FEA	Strip Width	FEA	Strip Width	FEA	Strip Width	FEA
Design Truck - Lane - Inventory	133.11	74.98	148.11	91.67	164.84	126.49	130.09	101.00
Design Tandem - Lane - Inventory	165.94	80.21	183.73	107.62	194.75	147.82	163.10	124.90
Design Truck - Lane - Operating	133.11	74.98	148.11	91.67	164.84	126.49	130.09	101.00
Design Tandem - Lane - Operating	165.94	80.21	183.73	107.62	194.75	147.82	163.10	124.90
AASHTO Type 3 Truck	100.13	52.05	109.52	66.26	114.84	87.45	97.28	74.99
AASHTO Type 3S2 Truck	91.28	47.49	103.38	59.75	111.67	72.01	91.92	70.12
AASHTO Type 3-3	82.47	42.90	90.17	54.55	94.46	85.53	80.11	61.69
AASHTO-notional	132.33	61.94	153.33	88.43	170.14	126.74	135.76	100.90
AASHTO-SU4	117.34	58.43	129.22	75.70	136.81	103.36	115.11	87.67
AASHTO-SU5	124.82	61.39	139.63	79.49	149.38	110.79	124.50	93.11
AASHTO-SU6	132.33	61.30	150.66	86.12	162.51	120.93	133.96	100.07
AASHTO-SU7	132.33	61.90	153.33	88.01	167.67	126.07	135.76	100.79
MaineDoT C1	132.69	64.79	147.19	84.46	156.38	116.55	131.11	97.54
MaineDoT C2	132.69	62.10	150.75	86.41	167.70	126.54	133.57	100.34
MaineDoT C3	132.69	62.02	147.19	84.61	156.38	116.70	131.11	97.55
MaineDoT C4	125.17	63.15	145.68	86.25	159.37	119.44	129.29	96.47
MaineDoT C5	134.60	71.69	146.57	90.51	156.11	119.67	130.47	101.31
MaineDoT C6	178.28	89.28	195.81	116.50	215.22	159.10	174.91	132.99
MaineDoT C7	144.08	74.04	162.05	97.58	174.27	133.31	144.58	110.94
MaineDoT C8	93.37	52.40	104.58	65.12	111.55	86.97	92.81	73.29
MaineDoT C9	143.01	83.55	156.76	100.17	174.25	135.71	137.57	110.84

Table 25 - Live Load Moments (kN – m/m) for Conventional Strip Width and Finite Element Analysis for Linneus Bridge #5311, Linneus Bridge #5773, Milford Bridge #2070 and Milo Bridge #2931.

	Monroe Bridge #5538		Newcastle Bridge #5608		Palmyra Bridge #5699		Sherman Bridge #2899	
Live Load Truck	Strip Width	FEA	Strip Width	FEA	Strip Width	FEA	Strip Width	FEA
Design Truck - Lane - Inventory	178.26	140.32	153.04	123.67	117.87	101.82	189.90	136.35
Design Tandem - Lane - Inventory	205.65	163.74	187.73	142.68	146.73	122.66	214.77	163.05
Design Truck - Lane - Operating	178.26	140.32	157.48	123.67	117.73	101.82	189.90	136.35
Design Tandem - Lane - Operating	205.65	163.74	187.73	142.68	146.73	122.66	214.77	163.05
AASHTO Type 3 Truck	120.55	96.74	110.98	85.18	88.60	74.09	127.80	95.47
AASHTO Type 3S2 Truck	119.26	94.89	107.16	81.83	80.79	67.55	124.86	93.22
AASHTO Type 3-3	99.28	79.68	91.41	71.61	72.97	60.75	103.07	78.47
AASHTO-notional	183.53	144.29	162.27	122.89	116.89	97.86	195.10	144.29
AASHTO-SU4	146.21	115.48	131.58	100.06	103.86	87.48	154.44	114.08
AASHTO-SU5	158.13	124.77	143.50	109.40	110.31	92.56	165.07	122.88
AASHTO-SU6	172.68	136.01	156.04	118.10	116.89	98.01	181.18	134.78
AASHTO-SU7	179.40	139.62	160.63	118.18	116.89	97.61	189.32	141.90
MaineDoT C1	164.90	129.45	150.39	113.44	117.24	95.97	171.88	128.29
MaineDoT C2	180.46	142.55	159.42	122.21	117.24	96.47	191.45	141.68
MaineDoT C3	164.90	131.66	150.39	113.74	117.24	96.44	176.15	130.69
MaineDoT C4	169.70	135.59	152.40	117.17	109.33	94.22	179.22	131.97
MaineDoT C5	165.30	132.93	149.95	120.06	119.18	101.64	173.12	130.86
MaineDoT C6	224.68	177.64	203.11	153.18	157.55	132.67	235.53	175.16
MaineDoT C7	184.38	147.13	166.90	128.66	127.45	107.29	192.79	143.21
MaineDoT C8	117.61	95.93	106.58	84.40	82.82	71.38	123.13	96.15
MaineDoT C9	187.27	153.27	166.19	132.41	126.69	110.55	198.97	149.91

6 Discussion of Results

The results show that the FEA model SlabRate increases the rating factors compared to the conventional strip width method by an average of 24.14% for non-skewed bridges, 48.12% for 15° skew bridges, 146.65% for 30° skew bridges and 299.75% for 45° skew bridges for all of the trucks. Similar increases were generally observed for the HL-93 design loadings, AASHTO legal loads, specialized hauling vehicles, and the MaineDoT rating trucks. These results indicate that finite element analysis is less conservative then the equivalent strip width method that is conventionally used in load rating.

Per the results of the SlabRate analyses, thirteen bridges that would have had an operating rating factor less than one and were at risk for posting based on the conventional strip width method had rating factors greater than one based on finite-element analysis. These bridges are Albion Bridge #2529, Argyle Township Bridge #3827, Brewer Bridge #5638, Carmel Bridge #5191, Carmel Bridge #5632, Exeter Bridge #5838, Greenfield Township Bridge #5605, Linneus Bridge #5311, Linneus Bridge #5773, Milford Bridge #2070, Monroe Bridge #5538, Newcastle Bridge #5608 and Palmyra Bridge #5699. Two bridges, Chester Bridge #5907 and Milo Bridge #2931 had rating factors greater than one using the conventional strip width method.

However, one issue that has not been sufficiently addressed is the effect of skew angle. The SlabRate analyses consider only longitudinal bending moments, and as skew angle increases, the transverse and torsional bending moments become more significant, which may lead to lower rating factors. Menassa et al. (2007) studied the effect of skew angle on slab analysis, concluding that the AASHTO provisions for predicting longitudinal bending moments can be very conservative for skew angles over 20 degrees, which is consistent with the results of this study. However, as discussed by Theorét et al. (2011), large skew angles can cause large transverse moments as well as shear forces that may govern capacity, and simplified code provisions must account for these transverse moments and shear forces. Denton and Burgoyne (1996) examined

the flexural assessment of reinforced concrete slabs with skewed reinforcement, proposing refined methods where skew is rigorously taken into account when determining bending strength.

The effect of skew angle is probably most pronounced for the Albion Bridge #2529, Brewer Bridge #5638, Carmel Bridge #5191, Carmel Bridge #5632, Linneus Bridge #5311, and Linneus Bridge #5773, which had skew angles greater than 20 degrees. Additional research will be required to assess the significance of skew angle and develop modified FE-based slab load rating procedures to better account for slab skew angle.

7 Summary and Conclusions

The main objective of this report was to determine the potential benefits of using the finite element method for load rating concrete slab bridges, and this report describes the finite-element load rating of twenty flab slab bridges in Maine.

The special-purpose finite-element program SlabRate, developed specifically for analyzing flat slab bridges, was used for the analyses. The finite-element formulation underlying SlabRate was validated through comparisons with both analytical solutions and commercial finite element software. One major advantage of using SlabRate for the finite element analysis instead of general-purpose finite element software is that the time to create the model is significantly less. SlabRate makes it very easy to input the bridge characteristics along with the number of elements and truck configurations, and solve for the maximum live load moments and rating factors. When using general-purpose FEA software, creating a model and considering multiple load cases are relatively time-consuming.

Both inventory and operating rating factors were determined for all twenty bridges. Both legal AASHTO live loadings and MaineDoT rating vehicles were used in all analyses, and rating factors were determined for all bridges and all vehicles based on both finite-element analysis and

the conventional AASHTO strip width method. The results of the load ratings show that thirteen bridges at risk for weight restrictions based on conventional strip width analysis have operating rating factors greater than one when rated using finite element analysis. However, of these thirteen bridges, six had skew angles exceeding 20 degrees. The finite-element based rating factors may be unrealistically high for these structures, since transverse and torsional moments which increase rapidly with large shear angles were not taken into account. Additional research will be required to fully assess the effect of skew angle.

8 References

AASHTO (2009). *Manual for Bridge Evaluation*. American Association of Highway and Transportation Officials, Washington, D.C.

AASHTO (2010). *LRFD Bridge Design Specifications*. American Association of Highway and Transportation Officials, Washington, D.C.

ANSYS Version 12.0.1(2009). http://www.ansys.com/Products/ (accessed 12/1/2010)

Abaqus/CAE Version 6.9 (2009). http://www.simulia.com/products/abaqus_fea.html (accessed 2/15/2)

Bhatti, A. (2006). *Advanced Topics in Finite Element Analysis of Structures*. John Wiley & Sons, New York, NY.

Denton, S.R. and Burgoyne, C.J. (1996). "The Assessment of Reinforced Concrete Slabs." *The Structural Engineer,* 74(9): 147-152.

Jáuregui, D.V., Licon-Lozano, A. and Kulkarni, K. (2007). "Improved Load Rating of Reinforced Concrete Slab Bridges." Report No. NM05STR-02, New Mexico Dept. of Transportation, Albuquerque, NM.

MaineDOT (2003), *Bridge Design Guide*. Maine Department of Transportation, Augusta, ME.

MaineDOT (2007), *Keeping Our Bridges Safe.* Maine Department of Transportation, Augusta, ME.

MaineDOT (2008), http://www.maine.gov/mdot/publicbridges/ (accessed 6/2010)

MathWorks (2009). http://www.mathworks.com/products/ (accessed 9/28/2009).

Menassa, C., Mabsout, M., Tarhini, K. and Frederick, G. (2007). "Influence of Skew Angle on Reinforced Concrete Slab Bridges." *Journal of Bridge Engineering*, 12(2): 205-214.

Théoret, P., Massicotte, B. and Conciatori, D. (2011). Analysis and Design of Straight and Skewed Slab Bridges. Journal of Bridge Engineering (in press, doi:10.1061/(ASCE)BE.1943-5592.0000249).

Timoshenko, S.P. and Woinowsky-Krieger, S. (1959). *Theory of Plates and Shells*. McGraw-Hill Book Company, New York, NY.

Load Rating Guideline for Flat Slab Concrete Bridges Using the Strip Width Method and Finite–Element Method

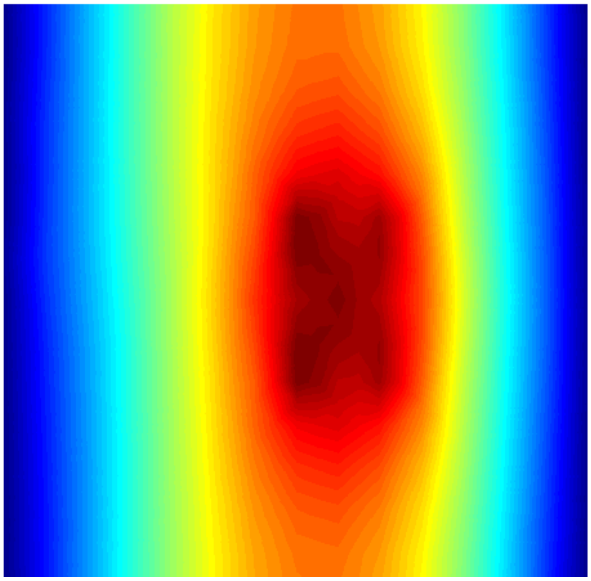

Authors:
William Davids Ph.D., P.E.
Timothy Poulin

1. Introduction

This document is a guide that draws on both accepted AASHTO and MaineDOT procedures and provides specific guidance for MaineDOT personnel and consultants performing load rating on flat concrete slab and rigid frame bridges. An overview of conventional load rating procedures is included as well as detailed guidance on the use of finite-element (FE) analysis techniques for concrete flat slab and rigid frame bridges. Examples of concrete slab bridge load ratings that demonstrate the application of conventional strip width and FE analysis methods are given at the end of the document.

Section 2 of this document overviews the conventional strip width method. These guidelines follow the 2008 edition of the AASHTO *Manual for Bridge Evaluation* (AASHTO 2008), along with the 2003 MaineDOT *Bridge Design Guide* with revisions from August 2008 (MaineDOT 2003). This document is to be used in conjunction with the current AASHTO *Manual for Bridge Evaluation*. This document also refers to specific sections in the AASHTO *Manual for Bridge Evaluation* for relevant information regarding the load rating of flat concrete slab bridges. The AASHTO *LRFD Bridge Design Specification* (AASHTO 2007) is also referred to extensively.

Section 3 provides guidance for the load rating of concrete slab bridges using finite-element analysis procedures. These guidelines are applied in conjunction with the 2008 edition of the AASHTO *Manual for Bridge Evaluation*.

Sections 4 and 5 of this document contain detailed examples of flat slab load rating using both the conventional strip width method and finite element analysis.

2. Conventional Slab Load Rating

Evaluation of Loads

General:

Loads for evaluation are determined with the use of section 6A.2 of the AASHTO Manual for Bridge Evaluation.

Only permanent loads and vehicular loads are considered to be of consequence in load rating. Environmental loads such as wind, ice, temperature, stream flow, and earthquake are usually not considered in rating except when unusual conditions warrant their inclusion. Creep and shrinkage also need not be evaluated if there is well-distributed reinforcement to control cracking (6A.2.3.8).

Dead Loads (DC and DW):

Dead loads should be computed in accordance to 6A2.2.1 of the AASHTO Manual for Bridge Evaluation.

DC: should be based on slab weight, curb weight and rail weight. The maximum moments at critical locations should be determined for a unit width. (i.e. units of kip-ft/ft, kN–m/m).
DW: should be based on the wearing surface and any utilities on the bridge. Maximum moments at critical locations should be determined per unit width (i.e. units of kip-ft/ft, kN–m/m).

Permanent Loads Other Than Dead Loads (P):

Permanent loads should be computed in accordance to 6A.2.2.2 of the AASHTO Manual for Bridge Evaluation.

Permanent loads P should be determined per unit width (i.e. units of kip-ft/ft, kN–m/m).

Transient Loads (LL):
Transient loads should be determined based on section 6A.2.3 of the AASHTO Manual for Bridge Evaluation.

The maximum moments should be determined by modeling the bridge as a beam, and dividing the maximum moment due to one lane of live loading by an equivalent strip width. Calculation of the equivalent strip width is discussed later in this document. If the bridge being rated is a simple span, Appendix E6A of the AASHTO Manual for Bridge Evaluation can be used to determine maximum moments for AASHTO trucks.

Design Live Loads: HL-93 Design Loads per the LRFD Design Specifications shall be used. The HL-93 loads include a design tandem, design truck and a lane load as well as an additional negative moment loading. The maximum moment caused by the design truck and design tandem must be multiplied by the Dynamic Load Allowance and added to the lane load moment, which does not include a Dynamic Load Allowance. The HL-93 truck axles and weights are given in appendix C6A.

Legal Live Loads: Legal live loads include AASHTO legal truck loads along with notional rating loads. The AASHTO legal truck loads are specified in Article 6A.4.4.2.1a of the AASHTO Manual for Bridge Evaluation, while the notional rating loads are specified in Article 6A.4.4.2.1b. All these loads will include dynamic load allowance factor. Axle spacing and weights can also be found in Appendix D6A of the AASHTO Manual for Bridge Evaluation.

Permit Live Load: Permit live loads are based on the specific permit truck.

Dynamic Load Allowance (IM):
Impact shall be evaluated as specified in Article 6A.2.3.3 of the AASHTO Manual for Bridge Evaluation.

The factor to be applied shall be taken as (1+IM/100), and is applied only axle loads, not lane loads. Generally IM shall be taken as 33% but can be modified according to C6A.4.4.3.

Evaluating Equivalent Strip

General:
Equivalent strip widths are determined in accordance with of the AASHTO LRFD Bridge Design Specifications.

The live load moments determined from the beam analysis must be divided by the equivalent strip width. The equivalent strip does not apply to the dead loads and the capacity of the bridge, but applies only to the live loads.

Skew Angle:
Equivalent strip widths for skewed bridges shall be reduced based on recommendations in the AASHTO LRFD Bridge Design Specifications.

Capacity of Bridge (Moment Resistance)
Concrete capacity shall be calculated in accordance with the AASHTO LRFD Bridge Design Specifications.

Maximum Reinforcement
The factored resistance of compression controlled prestressed and non-prestressed sections shall be reduced in accordance with the AASHTO LRFD Bridge Design Specifications.

Material Properties
If the concrete compressive strength f_c' is unknown then it may be estimated using Table 6A.5.2.1-1 of The AASHTO Manual for Bridge Evaluation. If the steel yield strength f_y is unknown, Table 6A.5.2.2-1 of the AASHTO Manual for Bridge Evaluation shall be used to determine a value for rating. Also section 6A.5 of the AASHTO Manual.

for Bridge Evaluation shall be used for reference for concrete. Alternatively, f_c' and f_y may be determined by testing material samples taken from the structure being rated. The strength reduction factor φ is determined by classifying sections as tension-controlled, transition, or compression-controlled.

Minimum Reinforcement
Concrete members that do not satisfy the minimum flexural reinforcement provisions of AASHTO LRFD Bridge Design Specifications shall have their strength reduced in accordance with 6A.5.7 of The Manual for Bridge Evaluation

Load Rating Equation

General:
The load rating should be determined in accordance of section 6A.4.2.1 of the AASHTO Manual for Bridge Evaluation. Equation 6A.4.2.1-1 shall be used to determine the rating factor, along with equations 6A.4.2.1-2 and 6A.4.2.1-3.

Rating factors shall be determined at critical locations. If the design level rating factors are below one, then the analyst must compute rating factors for the legal truck loads. If the minimum rating factors are still below one for legal loads posting must be considered per MaineDOT procedures.

Load Factors:
γ_{DC} shall be taken as 1.25 for reinforced concrete. (Table 6A.4.2.2-1). γ_{DW} shall be taken as 1.50, but if dimensions and materials are field verified 1.25 may be used. (Table 6A.4.2.2-1). γ_P shall be taken as 1.0 (Article 6A.2.2.3). γ_{LL} shall be taken from Table 6A.4.3.2.2-1. φ_C shall be determined from Table 6A.4.2.3-1 based on bridge inspections. 1.0 shall be used for φ_S (6A4.2.4-1). φ shall be determined as specified in AASHTO LRFD Design Bridge Design Specification as detailed above.

Design load factors for inventory and operating ratings are 1.75 and 1.35 respectively. Legal load factors shall be taken from Table 6A.4.4.2.3a-1 and be used for AASHTO truck loads and Table 6A.4.4.2.3b-1 for specialized hauling vehicles.

3. Slab Load Rating Using the Finite-Element Method

Construction of Finite Element Model

A finite element model of each bridge must be created. The finite element models can be created using solid, plate, or shell elements.

The model may assume

- Pin – pin boundary conditions,
- Linear elasticity
- Small deformations

Element performance should be verified by comparison with known analytical solutions for simple load cases. A Mesh refinement study must be performed to ensure convergence of the model. Skew angles may require the consideration of a combination of transverse and longitudinal bending moments

Extensive analyses have been done to verify these assumptions (Poulin 2012).

Evaluation of Loads

Same Loads will be evaluated as detailed in Section 2.

All loads should be determined with units of moment per length. (i.e. kN-m/m or lb-ft/ft

Application of Transient Live Loads

The application of vehicular live loads should be determined in accordance of section 6A.2.3.2 of the AASHTO Manual for Bridge Evaluation

Each axle loads should be evenly distributed between two wheel loads. Each wheel should be treated as a 10” by 20” uniform pressure.

Capacity of Bridge (Moment Resistance)

Capacity of the bridge is determined in the same manner as detailed in Section 2.

Load Rating Equation

The load rating equation is the same as detailed in Section 2.

4. Example Using Conventional Method

Flat Slab Concrete Bridge Example

Bridge Information:
Milford Bridge # 2070

Span Length:		27.349′ (centerline to centerline)
Span Width:		30.333′
Skew Angle:		15° (clockwise)
Slab Thickness:		16.5″
Wearing Surface Thickness:		4.5″ (concrete – average of 6″ and 3″ on drawings)
Curb Width:		14″ (both sides)
Curb Height (above slab):		12″ (both Sides)
ADTT(one direction):		unknown
Reinforcement:		#10 Bars (1.270″ diameter) at 6.5″ O.C.
Clear Cover:		1″
Material:	Concrete:	f'_c = 2.5 ksi (modular ratio of 10)
	Reinforced Steel:	f_y = 40 ksi (unknown bridge after 1954)

Dead Load Analysis

Components (DC)

Concrete slab

$$\frac{16.5}{12}\times 1\times 0.150 = 0.206 \text{ kip / ft}$$

Curb:

$$\frac{2\times\left(\frac{14}{12}\times\frac{12}{12}\right)\times 0.150}{30.33} = 0.012 \text{ kip/ft}$$

DC:

$$0.206 + 0.012 = 0.218 \text{ kip / ft}$$

M_{DC}:

$$M_{DC} = \frac{WL^2}{8} = 20.4 \text{ kip ft / ft}$$

Wearing Surface (DW)

Concrete wearing surface

$\frac{4.5}{12} \times 1 \times 0.150$ = 0.056 kip /ft

$M_{DW} = \frac{WL^2}{8}$ = 5.26 kip ft / ft

Live Load Analysis

Table 1 – Max Live Load Moments

Transient Load	Max Moment (M_{LL+IM})(Appendix E6A) kip-ft
Max Design Live Load (HL -93)	445
Type 3 truck unit	266
Type 3S2	259
Type 3-3	219
SU4	317
SU5	346
SU6	376
SU7	388
Notional Load	394

All values are maximum mid-span moments. Maximum design live load is the maximum moment cause by the either the truck or the tandem with dynamic load allowance factor. Lane load must be added to maximum moment, and the lane load does not include a dynamic load allowance factor.

Equivalent Strip Width

One Lane Loaded

$E = 10.0 + 5.0\sqrt{L_1 W_1}$

L_1 = Lesser of 27.3 ft or 60 ft = 27.4 ft

W_1 = Lesser of 30.3 ft or 30 ft = 30 ft

$E = 10.0 + 5.0\sqrt{27.3 \times 30}$

= 153 in

= 12.8 ft

Multilane Loaded

$E = 84.0 + 1.44\sqrt{L_1 W_1} \le \frac{12.0W}{N_L}$

L_1 = Lesser of 27.3 ft or 60 ft = 27.3 ft

W_1 = Lesser of 30.3 ft or 60 ft = 30.3 ft

$E = 84.0 + 1.44\sqrt{27.3 \times 30.3}$

= 126 in

= 10.5 ft

$N_L = \frac{30.3}{12} = 2$ Design Lanes

$\frac{12.0W}{N_L} = \frac{12.0 \times 30.3}{2} = 182 \text{ in} \geq 125 \text{ in}$ OK

Use E = 10.5 ft since 10.5 ft $\leq$ 12.8 ft

Skew Reduction Factor

$r = 1.05 - 0.25 \tan\theta$

$\theta = 15^{\circ}$ (clockwise)

$r = 1.05 - 0.25 \tan(15)$

$r = 0.983$

$E = r \times E$

$= 0.983 \times 10.5$

$= 10.3$ ft

Compute Capacity of Slab (Nominal Resistance)

$M_n = f_y \left(d - \frac{a}{2} \right)$

$c = \frac{A_s f_y}{0.85 f_c' b \beta_1}$

$A_s \quad \frac{1.27^2 \times \pi}{4} \times \frac{12}{6.5}$

$= 2.34 \text{ in}^2 / \text{ft}$

$\beta_1 = 0.85$

$b = 12$ in

$f_y = 40$ ksi

$f_c' = 2.5$ ksi

$c = \frac{2.34 \times 40}{0.85 \times 2.5 \times 12 \times 0.85}$

$= 4.3$

$a \quad \beta_1 c$

$= 0.85 \times 4.3$ in

$= 3.67$ in

d = Distance to CG of steel from compression face of concrete

$= 16.5 - 1 - \frac{1}{2} \times 1.27$

$= 14.9$ in

$M_n = 2.34 \times 40 \times \left(14.9 - \frac{3.67}{2} \right)$

= 1220 kip in / ft
= 102 kip ft / ft

Minimum Reinforcement (6A.5.7 of The Manual for Bridge Evaluation)
Amount of reinforcement must be sufficient to develop M_r equal to the lesser of:
$1.2M_{cr}$ or $1.33M_u$

M_r $= \varphi M_n = 0.90 \times 102$ kip ft
$= 91.4$ kip ft

1.) $1.33M_u$ $= 1.33 \times \left(1.75 \times \frac{445}{10.3} + 1.25 \times 20.4 + 1.25 \times 5.26 \right)$
$= 143$ kip ft > 91.4 No Good

2.) $1.2M_{cr}$ $= 1.2\left(S_c \left(f_r + f_{cpe} \right) - M_{dnc} \left(\frac{S_c}{S_{nc}} - 1 \right) \right) \geq 1.2\left(S_c f_r \right)$

Where a monolithic or composite section is designed to resist all the loads, S_{nc} is substituted for S_c. In this Case $f_{cpe} = 0$, therefore:

$1.2M_{cr}$ $= 1.2\left(S_{nc} f_r \right)$

S_{nc} $= \frac{I}{y_t}$

I = moment of inertia of uncracked section (neglecting reinforcement steel)
$= \frac{1}{12} \times 12 \times 16.5^3 = 4490 \text{ in}^4$

y_t = distance from neutral axis of the uncracked section to the extreme tension fiber
$= \frac{16.5}{2} = 8.25$ in

S_{nc} $= \frac{4490}{8.25} = 544 \text{ in}^3$

f_r $= 0.37\sqrt{f_c'} = 0.37\sqrt{3} = 0.585$ ksi

M_{cr} $= 0.585 \times 544 = 319$ kip in $= 26.5$ kip ft

$1.2M_{cr}$ $= 1.2 \times 26.5 = 31.9$ kip ft < 91.4 kip ft OK

The section meets the requirements for minimum reinforcement

Maximum Reinforcement (6A.5.6 of The Manual for Bridge Evaluation)
Current provisions of the LRFD specifications have eliminated the check for maximum reinforcement. Instead, the factored resistance (φ factor) of compression controlled sections shall be reduced in accordance with LRFD Design Article 5.5.4.2.1 This approach limits the capacity of over-reinforced (compression controlled) sections.

The net tensile strain ε_t is the tensile strain at nominal strength and determined by strain compatibility using similar triangles.

Given allowable concrete strain of 0.003 and depth to neutral axis c = 4.316 in (solved above):

$$\frac{\varepsilon_c}{c} = \frac{\varepsilon_t}{d-c}$$
$$\frac{0.003}{4.32} = \frac{\varepsilon_t}{14.9-4.32}$$

$\varepsilon_t = 0.00733$

For $\varepsilon_t = 0.00733 > .005$, the section is tension controlled and Resistance Factor φ shall be taken as 0.90

Shear

Concrete slabs and slab bridges designed in conformance with AASHTO specifications may be considered satisfactory for shear

Also shear need not be checked for design load and legal load ratings of concrete members.

General Load- Rating Equations (6A.4.2 of The Manual for Bridge Evaluation)

$$RF = \frac{c - (\gamma_{DC})(DC) - (\gamma_{DW})(DW) \pm (\gamma_P)(P)}{(\gamma_L)(LL+IM)} \qquad \text{Eq. 6A.4.2 – 1}$$

Evaluation of Factors (for Strength Limit States)

Resistance Factor, φ (LRFD Design 5.5.4.2)

φ = 0.90 For Flexure

Condition Factor, φ_c (6A.4.2.3)

φ_c = 1.0 No Deterioration

System Factor, φ_s (6A.4.2.4)

φ_s = 1.0 Slab Bridge

Design Load Rating (6A.4.3)

Strength I Limit State (6A.5.4.1)

$$RF = \frac{(\varphi)(\varphi_s)(\varphi_c)(R_n) - (\gamma_{DC})(DC) - (\gamma_{DW})(DW) \pm (\gamma_P)(P)}{(\gamma_L)\left(\frac{M_{LL+IM}}{E}\right)}$$

Load	Inventory	Operating	
γ_{DC}	1.25	1.25	
γ_{DW}	1.50	1.50	Asphalt was not field verified
γ_L	1.75	1.35	

Table 6A.4.2.2-1

Inventory:

$$RF = \frac{(0.9 \times 1.0 \times 1.0 \times 102) - (1.25 \times 20.4) - (1.50 \times 5.26) - (1.0 \times 0)}{\left(1.75 \times \frac{445}{10.3}\right)}$$

$$= 0.767$$

Operating:

$$RF = \frac{(0.9 \times 1.0 \times 1.0 \times 102) - (1.25 \times 20.4) - (1.50 \times 5.26) - (1.0 \times 0)}{\left(1.35 \times \frac{445}{10.3}\right)}$$

$$= 0.994$$

Service Limit State

No service limit states apply to reinforced concrete bridges.

As RF < 1.0 for HL-93, evaluate the bridge for Legal Loads.

Legal Load Rating (6A.4.4)

Live Loads: AASHTO Legal Trucks – Type 3, Type 3S2, Type 3-3

(6A.4.4.2.1) Specialized Hauling Vehicles – SU4, SU5, SU6, SU7, Notional Rating

E = 10.278

IM = 33% (Unknown riding surface)

	Type 3	Type 3S2	Type 3-3	SU4	SU5	SU6	SU7	Notional
M_{LL+IM} (kip ft)	266	259	219	317	346	376	388	394
$\frac{M_{LL+IM}}{E}$ (kipft/ft)	25.8	25.2	21.3	30.8	33.6	36.6	37.8	38.3

Strength I Limit State (6A.5.4.2.1)

For AASHTO Trucks:

ADTT =Unknown

γ_L = 1.80

$$RF = \frac{(0.9 \times 1.0 \times 1.0 \times 102) - (1.25 \times 20.4) - (1.50 \times 5.26) - (1.0 \times 0)}{\left(1.80 \times \frac{M_{LL+IM}}{E}\right)}$$

For Specialized Hauling Vehicles:
ADTT = Unknown
γ_L = 1.60

$$RF = \frac{(0.9 \times 1.0 \times 1.0 \times 102) - (1.25 \times 20.4) - (1.50 \times 5.26) - (1.0 \times 0)}{\left(1.60 \times \frac{M_{LL+IM}}{E}\right)}$$

	Type 3	Type 3S2	Type 3-3	SU4	SU5	SU6	SU7	Notional
RF	1.25	1.28	1.52	1.18	1.08	0.992	0.961	0.947

No Posting required as RF> 1.0 for all AASHTO Legal Loads

Service Limit State

No service limit states apply to reinforced concrete bridge members at the Legal Load Rating.

Shear

Concrete slab and slab bridges designed in conformance with AASHTO specifications may be considered satisfactory for shear. Shear need not be checked for legal loads

5. Example Using the Finite-Element Method

Flat Slab Concrete Bridge Example

Bridge Information:
Milford Bridge # 2070

Span Length:		27.3′ (Centerline to Centerline)
Span Width:		30.3′
Skew Angle:		15° (clockwise)
Slab Thickness:		16.5″
Wearing Surface Thickness:		4.5″ (Concrete Surface) (Average of 6″ and 3″)
Curb Width:		14″ (Both sides)
Curb Height (above slab):		12″ (Both Sides)
ADTT(one direction):		Unknown
Reinforcement:		#10 Bars (1.270″ Diameter Bars) at 6.5″ O.C.
Clear Cover:		1″
Material:	Concrete:	f'_c = 2.5 ksi (Modular Ratio of 10)
	Reinforced Steel:	f_y = 40 ksi (Unknown Bridge after 1954)

Finite Element Model Details
The finite element model was constructed with 8-noded, shear deformable plate elements which are described in some detail in Bhatti (2006). Quadratic shape functions were used to interpolate element displacements. Shear contributions to the element stiffness matrix are under-integrated using 2x2 Gaussian quadrature, and 3x3 Gaussian quadrature is used for integrating the bending contributions to the element stiffness matrix. An isoparametric element formulation was used to allow the use of non-rectangular elements and accommodate skewed supports. Pinned supports, linearly elastic materials and small deformations were assumed in the analysis.

A mesh refinement study was conducted to ensure convergent and accurate results. The mesh refinement study relied on uniform meshes, and examined the effects of both the number of longitudinal and transverse elements used in the model on the maximum live load moments due to the HL-93 tandem truck with lane load. The truck was placed at the position on the bridge that provided the maximum moment. Dead load moments converged at lower levels of mesh refinement than live loads.

Figure 1 shows a plan view of the finite-element mesh with 14 by 14 elements. The elements adjacent to the top and bottom slab edges are thinner because two elements are used from the slab edge to the point nearest the curb at which the load can be positioned. The top and bottom row of elements correspond to the curb width of 14 inches. The elements just inside of those correspond to the 24 inch width that the truck cannot be placed within to satisfy the AASHTO requirement that no wheel be placed closer than 24” from a curb. The rest of the elements have a width of 28.8 inches.

Figure 2 is a plot of max moments vs. number of transverse elements to ensure convergence of the model. Each line on the graph represents different amount longitudinal elements. As can be seen from the graph, the models converge to a consistent value around 14 longitudinal and transverse elements. All the mesh sizes more refined than 14 longitudinal and 14 transverse elements provide results within 0.5% of the 14 by 14 mesh. The skew angle of 15 degrees is considered small enough that the analysis can be based only on longitudinal bending moments.

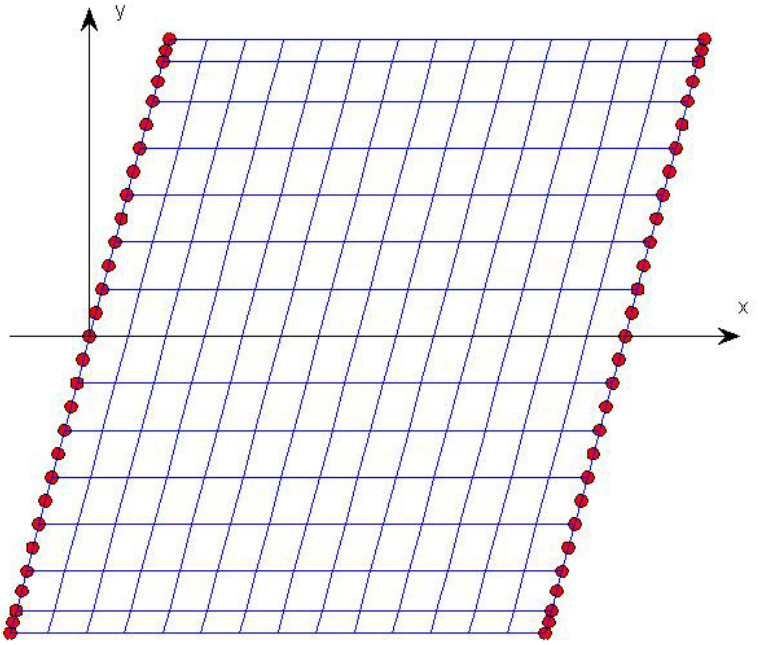

Figure 1 – Typical Finite-Element Mesh

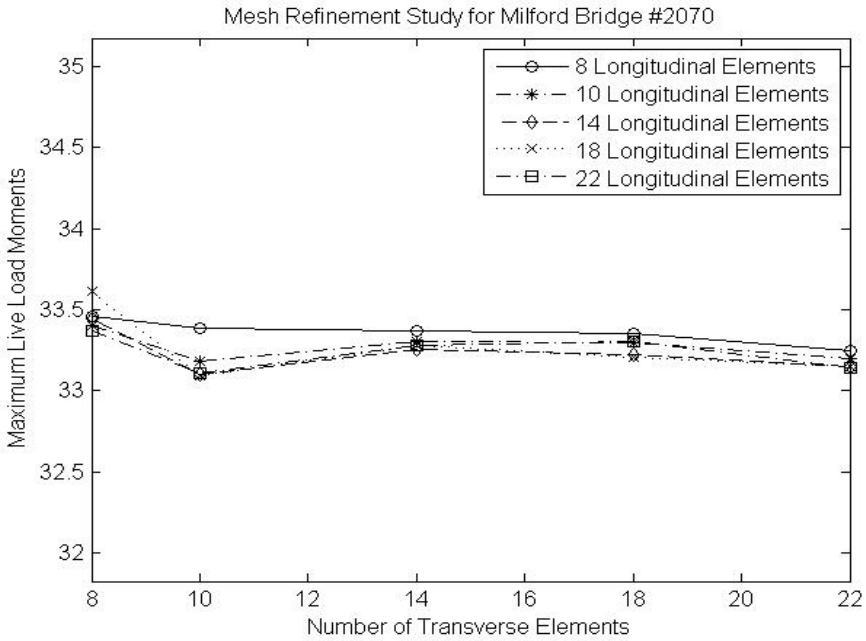

Figure 2 – Results of Mesh Refinement Study

Dead Load Analysis
The curb weights are treated as uniform pressures acting over the width of each curb along the span of the bridge. The slab weight was treated as a uniform pressure that acts over the entire bridge, and the wearing surface was treated as a uniform pressure acting between the curb faces.

Tables 2 and 3 give the dead load moments at the location of the maximum live load moment. These values are given for each rating vehicle because the location of maximum live load moment varies with truck type.

Table 2 – DC Moments at Location of the Maximum LL Moment

Transient Load	Max Moment (M_{DC}) kip-ft / ft
Max Design Live Load(HL -93)	19.0
Type 3 truck unit	19.0
Type 3S2	19.0
Type 3-3	19.7
SU4	19.0
SU5	19.0
SU6	19.7
SU7	19.7
Notional Load	19.7

Table 3 – DW Moments at Location of the Maximum LL Moment

Transient Load	Max Moment (M_{DW}) kip-ft /ft
Max Design Live Load(HL -93)	4.11
Type 3 truck unit	4.11
Type 3S2	4.11
Type 3-3	4.21
SU4	4.11
SU5	4.11
SU6	4.21
SU7	4.21
Notional Load	4.21

Live Load Analysis
Figure 3 shows the placement of the HL-93 Tandem Load which resulted in the maximum moment for all the different load combinations. Not shown is the lane load that acts over a ten foot loaded width positioned transversely within each lane. The center of the lane load is centered on the center of the truck. Each truck is considered to be a lane so there are two lane loads applied in Figure 3, one for each lane. The location to the center of the bottom truck's back axle is (103.0, -108.0) inches from center of the left pier in the *x*-*y* coordinate system indicated in Figure 3. The vertical spacing of the trucks is 6 ft from the center of the top wheels of the bottom truck to the center of the bottom wheels of the top truck. An *x*-position offset was used to place the truck at the same relative

distance away from the supports. This was done by placing the trucks at the same skew angle of the bridge.

Table 4 shows the maximum live load moments produced by each rating vehicle. The table provides the maximum moment, where the maximum moment occurs and the location and direction of the truck that produces the maximum moment.

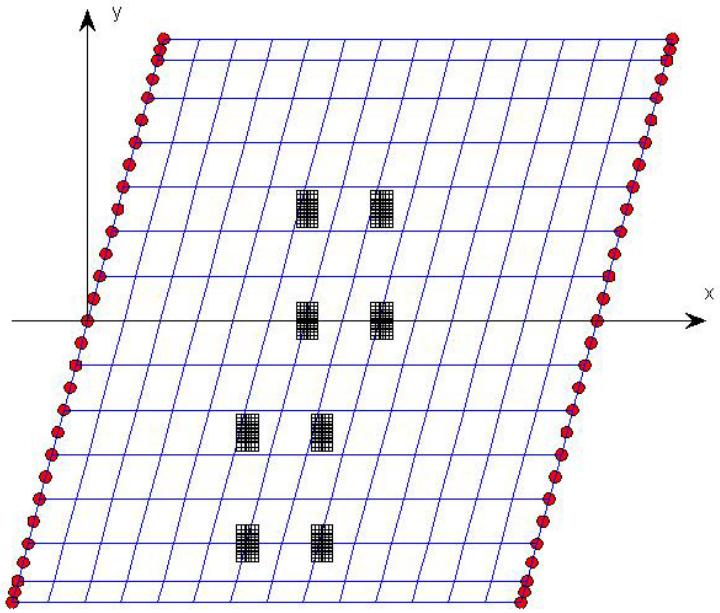

Figure 3 – Placement of the HL-93 Tandem to Maximize Live Load Moment

Table 4 – Maximum Live Load Moments including Dynamic Load Allowance

Transient Load	Max Moment (M_{LL+IM}) kip-ft / ft	Location of Maximum Moment (inches)	Location of Truck at Max Moment (inches)	Number of Lanes	Direction of Truck
Max Design Live Load (HL -93)	33.3	(149.0, -144)	(103.0, -108.0)	2	Right
Type 3 truck unit	19.7	(149.0, -144.0)	(148.6, -108.0)	2	Left
Type 3S2	19.0	(125.5, -144.0)	(-236.9, -108.0)	2	Right
Type 3-3	16.2	(140.6, -175.0)	(107.3, -108.0)	2	Right
SU4	23.3	(125.5, -144.0)	(73.2, -108.0)	2	Right
SU5	25.1	(125.5, -144.0)	(78.7, -108.0)	2	Right
SU6	27.2	(140.6, -175.0)	(48.4, -108.0)	2	Right
SU7	28.4	(140.6, -175.0)	(6.6, -108.0)	2	Right
Notional Load	28.5	(140.6, -175.0)	(298.0, -108.0)	2	Left

All loads reported generate the lowest rating factor for each specific truck type. The truck positions are the distance to the center of the back axle of the bottom truck to the center of the left pier. For the spacing of multiple trucks the center of the closest wheels are placed 6 ft away from each other per AASHTO. The trucks are also offset in the traffic

direction based on the skew of the bridge, which leads to each wheel being at the same relative distance away from the pier in the span direction.

Compute Capacity of Slab (Nominal Resistance)
Capacity calculations are given in section 4.

General Load- Rating Equations (6A.4.2 of The Manual for Bridge Evaluation)

$$RF = \frac{C - (\gamma_{DC})(DC) - (\gamma_{DW})(DW) \pm (\gamma_p)(P)}{(\gamma_L)(LL + IM)} \qquad \text{Eq. 6A. 4.2. } -1$$

Evaluation of Factors (for Strength Limit States)

Resistance Factor, φ (LRFD Design 5.5.4.2)

φ = 0.90 For Flexure

Condition Factor, φ_c (6A.4.2.3)

φ_c = 1.0 No Deterioration

System Factor, φ_s (6A.4.2.4)

φ_s = 1.0 Slab Bridge

Design Load Rating (6A.4.3)

Strength I Limit State (6A.5.4.1)

$$RF = \frac{(\varphi)(\varphi_S)(\varphi_C)(R_n) - (\gamma_{DC})(DC) - (\gamma_{DW})(DW) \pm (\gamma_P)(P)}{(\gamma_L)\left(\frac{M_{LL+IM}}{E}\right)}$$

Load	Inventory	Operating	
γ_{DC}	1.25	1.25	
γ_{DW}	1.50	1.50	Asphalt thickness not field verified
γ_L	1.75	1.35	

Table 6A.4.2.2-1

Inventory:

$$RF = \frac{(0.9 \times 1.0 \times 1.0 \times 102) - (1.25 \times 19.0) - (1.50 \times 4.11) - (1.0 \times 0)}{(1.75 \times 33.3)}$$

$$= 1.05$$

Operating:

$$RF = \frac{(0.9 \times 1.0 \times 1.0 \times 102) - (1.25 \times 19.0) - (1.50 \times 4.11) - (1.0 \times 0)}{(1.35 \times 33.3)}$$

$= 1.36$

Service Limit State

No service limit states apply to reinforced concrete bridges.

Since RF > 1.0 for HL-93, evaluation of the bridge for legal loads is not needed. Legal load rating is done here only as an example.

Legal Load Rating (6A.4.4)

Live Loads: AASHTO Legal Trucks – Type 3, Type 3S2, Type 3-3

(6A.4.4.2.1) Specialized Hauling Vehicles – SU4, SU5, SU6, SU7, Notional Rating

	Type 3	Type 3S2	Type 3-3	SU4	SU5	SU6	SU7	Notional
M_{LL+IM} (kip ft/ft)	19.7	19.0	16.2	23.3	25.1	27.2	28.4	28.5
M_{DC} (kip ft/ft)	19.0	19.0	19.7	19.0	19.0	19.7	19.7	19.7
M_{DW} (kip ft/ft)	4.11	4.11	4.21	4.11	4.11	4.21	4.21	4.21

Strength I Limit State (6A.5.4.2.1)

For AASHTO Trucks:

ADTT =Unknown

$\gamma_L = 1.80$

$$RF = \frac{(0.9 \times 1.0 \times 1.0 \times 102) - (1.25 \times M_{DC}) - (1.50 \times M_{DW}) - (1.0 \times 0)}{(1.80 \times M_{LL+IM})}$$

For Specialized Hauling Vehicles:

ADTT = Unknown

$\gamma_L = 1.60$

$$RF = \frac{(0.9 \times 1.0 \times 1.0 \times 102) - (1.25 \times M_{DC}) - (1.50 \times M_{DW}) - (1.0 \times 0)}{(1.60 \times M_{LL+IM})}$$

	Type 3	Type 3S2	Type 3-3	SU4	SU5	SU6	SU7	Notional
RF	1.72	1.78	2.06	1.64	1.52	1.38	1.32	1.32

No Posting required as RF> 1.0 for all AASHTO Legal Loads

An average increase in rating factor of 38.2% was seen going from the strip width method to the finite element method for this bridge. This was predominantly caused by the maximum live load moments decreasing by an average of 24.5% going from strip width method to the finite element models. Even though this specific bridge does not go from a rating factor below one for the strip width method to above one using the finite element method, it could happen with this larger increase in rating factors.

6. References

AASHTO (2008). *Manual for Bridge Evaluation*. American Association of Highway and Transportation Officials, Washington, D.C.

AASHTO (2007). *LRFD Bridge Design Specifications*. American Association of Highway and Transportation Officials, Washington, D.C.

Bhatti, A. (2006). *Advanced Topics in Finite Element Analysis of Structures*. John Wiley & Sons, New York, NY.

MaineDOT (2003), *Bridge Design Guide*. Maine Department of Transportation, Augusta, ME.

Poulin, T.J. (2012). "Development of Improved Load Rating Procedures and Retrofitting Techniques for Flat Slab Bridges." M.S. thesis, Dept. of Civil and Environmental Engineering, University of Maine.